Electronic Supplementary Information (ESI)

Aggregation-enhanced TADF in deep-red emitters for high-performance OLEDs

Chengrui Huang, Jianping Zhou, Kerim Samedov, Liang Zhang, Guoqing Peng, Xiangchao Peng, Mingxing Chen, Dongdong Zhang and Yuanjing Cai**

C. Huang, J. Zhou and K. Samedov contributed equally.

[a] C. Huang, Dr. K. Samedov, L. Zhang, G. Peng, X. Peng, Prof. Y. Cai
Beijing Advanced Innovation Center for Soft Matter Science and Engineering,
Beijing University of Chemical Technology,
Beijing, 100029 P. R. China
E-mail:gardencyj@hotmail.com

[b] J. Zhou, Prof. D. Zhang
Key Laboratory of Organic Optoelectronics & Molecular Engineering of Ministry of Education,
Department of Chemistry,
Tsinghua University,
Beijing, 100084 P. R. China
E-mail: ddzhang@mail.tsinghua.edu.cn

[c] Dr. M. Chen
Analytical Instrumentation Center,
Peking University,
Beijing, 100871 P. R. China

Table of Contents

Materials

All solvents and reagents were purchased from Sigma Aldrich and used without further purification unless otherwise stated. Tetrahydrofuran (THF) was distilled from sodium benzophenone ketyl radical under dry oxygen-free argon immediately before use.

1. Synthetic Procedures

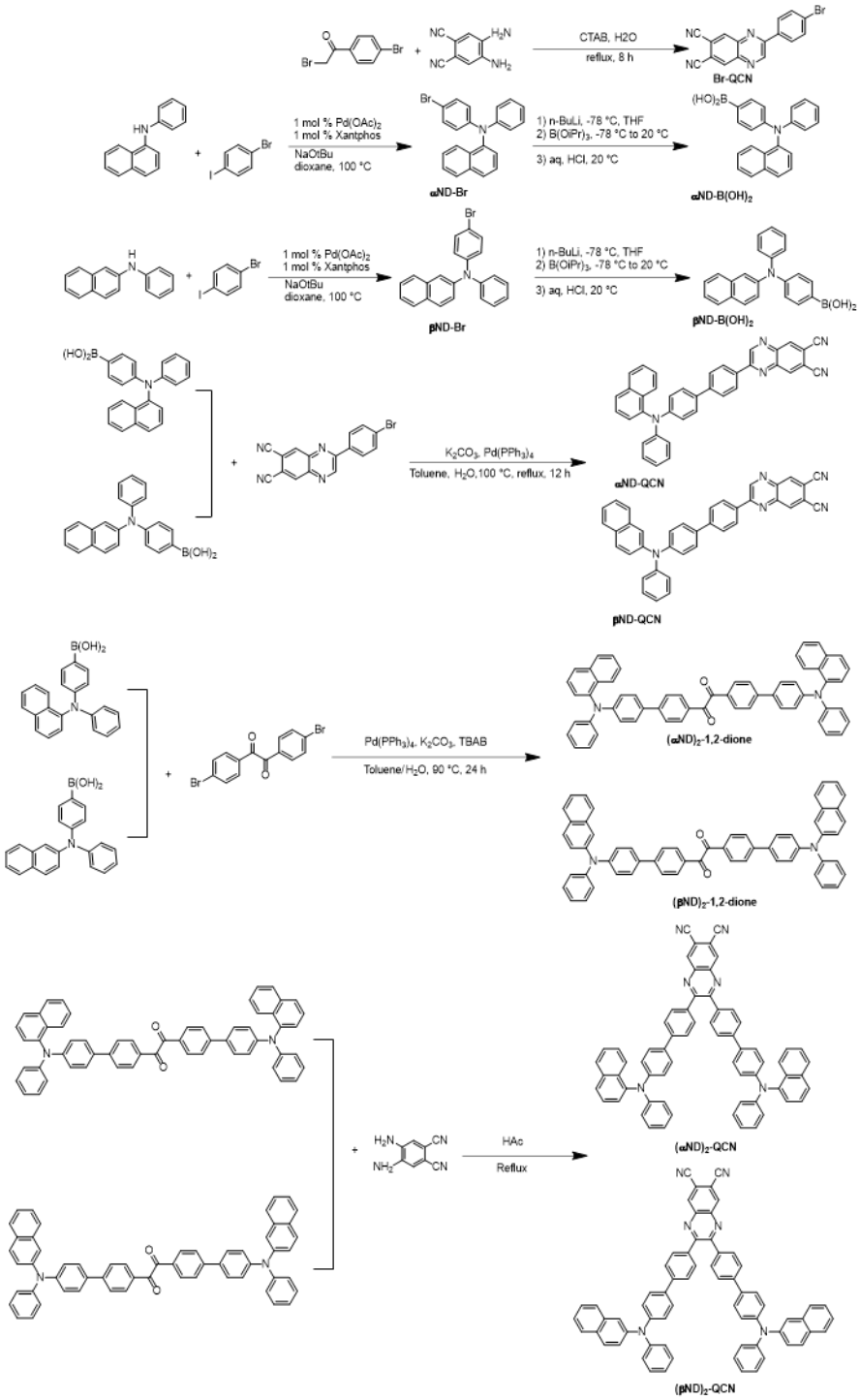

Scheme S1. Synthetic routes to quinoxaline-6,7-dicarbonitrile derivatives.

Synthesis of 2-(4-bromophenyl)quinoxaline-6,7-dicarbonitrile (Br-QCN) [1]: A 250 mL two-necked round bottom flask with a stir bar was fitted with a reflux condenser. The system was evacuated and filled with nitrogen three times. Under nitrogen atmosphere, 2-bromo-1-(4-bromophenyl)ethan-1-one (2.80 g, 10.0 mmol), 4,5-diaminophthalonitrile (1.90 g, 12.0 mmol), hexadecyltrimethylammonium bromide (CTAB, 0.90 g, 2.50 mmol) and deionized H_2O (50 mL) were added sequentially. After refluxing for 12 h, deionized water (15 mL) was added and the reaction mixture was extracted three times dichloromethane/ H_2O (1:1) and then the organic layers were separated, dried over anhydrous $MgSO_4$, filtered, and concentrated *in vacuo*. The crude product was purified by column chromatography with a dichloromethane/petroleum ether (1:1) mixture as an eluent to yield the target compound, 2-(4-bromophenyl)quinoxaline-6,7-dicarbonitrile (**Br-QCN**), as a yellow powder (1.10 g, yield: 33 %).^{1}H NMR (400 MHz, chloroform-*d*): δ = 9.52 (s, 1H), 8.62 (s, 1H), 8.61 (s, 1H), 8.15 (d, ^3J = 8.6 Hz, 2H), 7.77 (d, ^3J = 8.6 Hz, 2H) ppm.

Synthesis of N-phenyl-N(1-naphthyl)-4-bromoaniline (αND-Br) [2]: A 250 mL two-necked round bottom flask with a stir bar was fitted with a reflux condenser. The system was evacuated and filled with nitrogen three times. Under nitrogen atmosphere, 1-naphthylaminobenzene (1.00 g, 4.57 mmol), 1-bromo-4-iodobenzene (1.55 g, 5.48 mmol), palladium (II) acetate (10.25 mg, 0.046 mmol), 4,5-bis (diphenylphosphine)-9,9-dimethylxanthene (26.39 mg, 0.046 mmol), sodium tert-butoxide (0.65 g, 6.87 mmol,) and dioxane (30 mL) were added. The resulting reaction mixture was refluxed for 12 hours. After that, the reaction mixture was extracted three times with dichloromethane/H_2O (1:1), the organic layers were separated, combined dried over anhydrous $MgSO_4$, filtered, and concentrated *in vacuo.* The crude product was purified by column chromatography with a dichloromethane/petroleum ether (1:15) mixture as an eluent to give the product, *N*-phenyl-*N*(1-naphthalenyl)-4-bromoaniline (**αND-Br**), as a white solid (1.20 g, yield: 71 %).^{1}H NMR (400 MHz, chloroform-*d*): δ = 7.98 (d, ^3J = 8.6 Hz, 1H), 7.95 (d, ^3J = 8.3 Hz, 1H), 7.85 (d, ^3J = 8.2 Hz, 1H), 7.55-7.51 (m, 2H), 7.43 (dd, ^3J = 8.3 Hz, 6.8 Hz, 1H), 7.38 (d, ^3J = 7.3 Hz, 1H), 7.33 (d, ^3J = 8.8 Hz, 2H), 7.29-7.25 (m, 2H), 7.13 (d, ^3J = 7.3 Hz, 2H), 7.04 (t, ^3J = 7.3 Hz, 2H), 6.95 (d, ^3J = 8.8 Hz, 2H) ppm.

Synthesis of (4-(naphthalen-1-yl(phenyl)amino)phenyl) boronic acid (αND-B(OH)$_2$) [3]: A 250 mL two-necked round bottom flask with a stir bar was fitted with an inlet Schlenk adapter. The system was evacuated and filled with nitrogen three times. Under a nitrogen

atmosphere, N-phenyl-N(1-naphthyl)-4-bromoaniline (4.60 g, 12.30 mmol) was added to the flask, dissolved in anhydrous THF (80 mL) and cooled to -78°C. n-BuLi (2.5 M in hexane, 5.90 mL, 14.80 mmol) was added dropwise slowly while stirring. After completing the addition, the reaction mixture was stirred for another hour at -78 °C. Then, triisopropyl borate (4.64 g, 5.7 mL, 24.70 mmol) was added in one portion. The reaction mixture was stirred at room temperature for 14 h. The reaction was quenched afterward with a ca. 2 M aqueous HCl solution. The quenched reaction mixture was extracted with dichloromethane (DCM)/water (1:1). After repeating the operation three times, the organic layers were separated, combined, dried over anhydrous $MgSO_4$, filtered, and concentrated *in vacuo*. The crude product was purified by trituration with dichloromethane and subsequent precipitation with petroleum ether to give pure ((4-(naphthalen-1-yl(phenyl)amino)phenyl) boronic acid (**αND-B(OH)$_2$**) (3.14 g, yield: 75 %).^{1}H NMR (400 MHz, chloroform-*d*): δ = 7.94-7.88 (m, 4H), 7.80 (d, ^3J = 8.2 Hz, 1H), 7.54-7.44 (m, 2H), 7.36 (d, ^3J = 7.4 Hz, 2H), 7.23 (d, ^3J = 7.4 Hz, 2H), 7.17 (d, ^3J = 7.3 Hz, 2H), 7.02 (t, ^3J = 7.30 Hz, 1H), 6.97 (d, ^3J = 7.3 Hz, 2H) ppm.

Synthesis of N-phenyl-N(2-naphtalenyl)-4-bromoaniline (βND-Br): A 250 mL two-necked round bottom flask with a stir bar was fitted with a reflux condenser. The system was evacuated and filled with nitrogen three times. Under nitrogen atmosphere, N-phenylnaphthalen-2-amine (1.00 g, 4.57 mmol), 1-bromo-4-iodobenzene (1.55 g, 5.48 mmol), palladium (II) acetate (10.3 mg, 0.046 mmol), 4,5-bis(diphenylphosphino)-9,9-dimethyloxanthene (26.4 mg, 0.046 mmol), sodium tert-butoxide (0.65 g, 6.87 mmol), dioxane (30 mL) were added. The reaction mixture was refluxed for 12 hours. After that, the reaction mixture was extracted three times with dichloromethane/H_2O (1:1), the organic layers were combined, dried over anhydrous $MgSO_4$, filtered, and concentrated *in vacuo*. The crude product was then purified by column chromatography with a dichloromethane/petroleum ether (1:15) mixture as an eluent to give the product, N-phenyl-N(2-naphthalenyl)-4-bromoaniline (**βND-Br**), as a white solid (1.18 g, yield: 70 %). ^{1}H NMR (400 MHz, chloroform-*d*): δ = 7.80 (d, ^3J = 7.8 Hz, 1H), 7.77 (d, ^3J = 8.8 Hz, 1H), 7.64 (d, ^3J = 8.8 Hz, 1H), 7.47-7.42 (m, 3H), 7.39 (d, ^3J = 8.8 Hz, 2H), 7.34 -7.28 (m, 3H), 7.17 (d, ^3J = 7.3 Hz, 2H), 7.11 (t, ^3J = 7.3 Hz, 1H), 7.04 (d, ^3J = 8.8 Hz, 2H) ppm.

Synthesis of (4-(naphthalen-2-yl(phenyl)amino) phenyl) boronic acid (βND-B(OH)$_2$): A 250 mL two-necked round bottom flask with a stir bar was fitted with an inlet Schlenk

adapter. N-phenyl-N(2-naphthyl)-4-bromoaniline (4.60 g, 12.30 mmol) was added to the flask, dissolved in anhydrous THF (80 mL), and cooled to -78 °C under a nitrogen atmosphere. n-BuLi (2.5 M in hexane, 5.90 mL, 14.80 mmol) was added dropwise slowly while stirring. After completion of the addition, the mixture was stirred at -78 °C for another 1 h. Thereafter, triisopropyl borate (4.64 g, 5.70 mL, 24.70 mmol) was added in one portion. The reaction mixture was stirred at room temperature for 14 h. Finally, the reaction was quenched with a ca. 2 M HCl aqueous solution. The quenched reaction mixture was extracted with dichloromethane /water (1:1). After repeating the operation three times, the organic layers were separated, combined, dried over anhydrous $MgSO_4$, filtered, and concentrated *in vacuo*. An attempt was made to purify the crude product by trituration with dichloromethane and subsequent precipitation with petroleum ether. A white solid (3.06 g) was obtained. It was identified by ^{1}H NMR spectroscopy as a mixture of the desired product, (4-(naphthalen-2-yl(phenyl)amino) phenyl) boronic acid (**βND-B(OH)$_2$**), and an intractable impurity. Subsequent attempts to purify the compound were unsuccessful. The crude material was used in the next step without purification.

Synthesis of 1,2-bis(4'-(naphthalen-1-yl(phenyl)amino)-[1,1'-biphenyl]-4-yl) ethane-1,2-dione ((αND)$_2$-1,2-dione): A 250 mL two-necked round bottom flask with a stir bar was fitted with a reflux condenser. Under nitrogen atmosphere, 1,2-bis(4-bromophenyl)ethane-1,2-dione (1.00 g, 2.70 mmol), (4-(naphthalen-1-yl(phenyl)amino) phenyl) boronic acid (2.80 g, 8.10 mmol), tetrakis(triphenylphosphine)palladium (92 mg, 0.08 mmol), potassium carbonate (3.4 g, 24.30 mmol), toluene (75 mL), H_2O (25 mL) and tetrabutylammonium bromide (261 mg, 0.8 mmol) were added in sequence. The reaction mixture was stirred at 90 °C for 24 hours. Then, it was quenched with deionized water (15 mL), and the quenched reaction mixture was extracted three times with dichloromethane/water (1:1). The organic layers were separated, combined, dried over anhydrous $MgSO_4$, filtered, and concentrated *in vacuo*. The crude product was purified by column chromatography with a tetrahydrofuran: petroleum ether (1:10) mixture as an eluent to yield the target compound, **(αND)$_2$-1,2-dione**, as an orange powder (1.68 g, yield: 78 %). ^{1}H NMR (400 MHz, chloroform-*d*): δ = 8.00 (d, ^3J = 8.4 Hz, 4H), 7.93 (d, ^3J = 8.8 Hz, 2H), 7.91 (d, ^3J = 8.8 Hz, 2H), 7.81 (d, ^3J = 8.2 Hz, 2H), 7.66 (d, ^3J = 8.4 Hz, 4H), 7.52-7.45 (m, 8H), 7.40-7.36 (m, 4H), 7.23 (d, ^3J = 7.2 Hz, 4H), 7.14 (d, ^3J = 7.4 Hz, 4H), 7.03 (d, ^3J = 7.4 Hz, 4H), 7.00 (t, ^3J = 7.2 Hz, 2H) ppm.

Synthesis of 1,2-bis(4'-(naphthalen-2-yl(phenyl)amino)-[1,1'-biphenyl]-4-yl)ethane-1,2-dione ((βND)$_2$-1,2-dione): A 250 mL two-necked round bottom flask with a stir bar was fitted with a reflux condenser. Under nitrogen atmosphere, 1,2-bis(4-bromophenyl)ethane-1,2-dione (1.00 g, 2.70 mmol), (4-(naphthalen-2-yl(phenyl)amino) phenyl) boronic acid (2.80 g, 8.10 mmol), tetrakis(triphenylphosphine)palladium (92 mg, 0.08 mmol), potassium carbonate (3.40 g, 24.30 mmol), toluene (75 mL), H_2O (25 mL) and tetrabutylammonium bromide (261 mg, 0.80 mmol) were added in sequence. The reaction mixture was stirred at 90 °C for 24 hours. Then, it was quenched with deionized water (15 mL), and the quenched reaction mixture was extracted three times with dichloromethane/water (1:1). The organic layers were separated, combined, dried over anhydrous $MgSO_4$, filtered, and concentrated *in vacuo*. The crude product was purified by column chromatography with a tetrahydrofuran: petroleum ether (1:10) mixture as an eluent to yield the target compound, **(βND)$_2$-1,2-dione**, as an orange powder (1.70 g, yield: 79 %). ^{1} NMR (400 MHz, chloroform-*d*): δ = 8.05 (d, ^3J = 8.5 Hz, 4H), 7.79-7.71 (m, 8H), 7.63 (d, ^3J = 7.2 Hz, 2H), 7.54 (d, ^3J = 8.5 Hz, 4H), 7.52-7.51 (d, J = 2.2 Hz, 2H), 7.44-7.37 (m, 4H), 7.33-7.29 (m, 6H), 7.20-7.18 (m, 8H), 7.11 (t, ^3J = 7.3 Hz, 2H) ppm.

2. NMR and MALDI-TOF-MS Spectra:

^{1}H and $^{13}C\{^{1}H\}$ NMR spectra were measured on an AVANCE III HD 400 MHz spectrometer. Resonance of the residual traces of the protonated NMR solvent was used to reference the spectra. Mass spectra were recorded on a Shimadzu Biotech GC/MS mass spectrometer operating in a matrix-assisted laser desorption ionization time-of-flight mode.

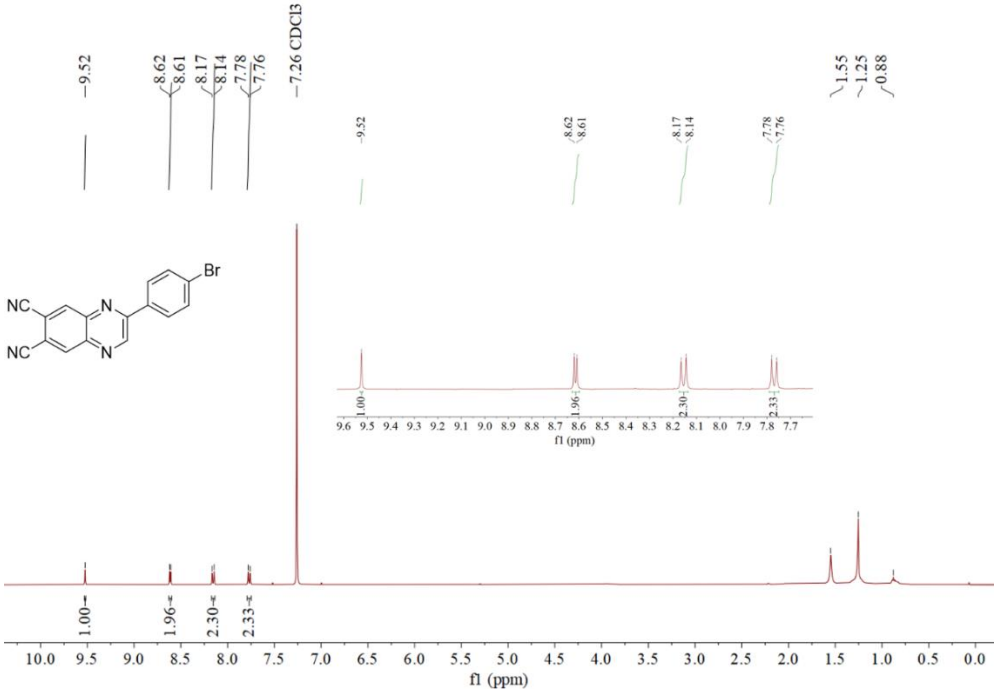

Figure S1. ^{1}H NMR spectrum of compound **Br-QCN**.

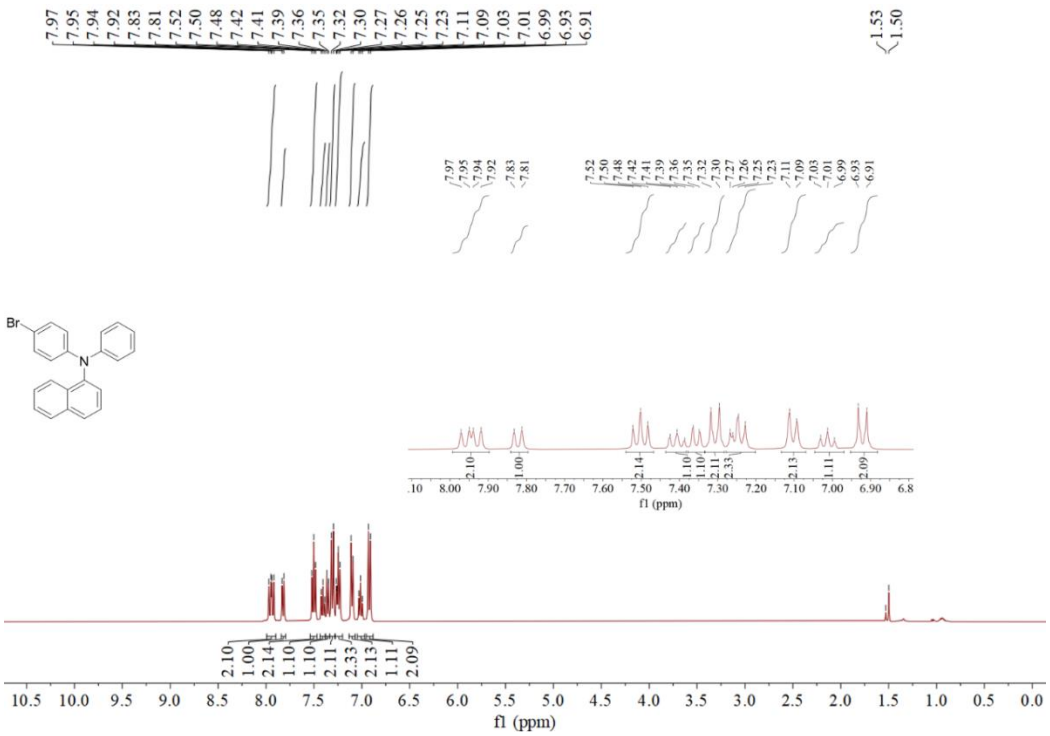

Figure S2. ^{1}H NMR spectrum of compound **αND-Br**.

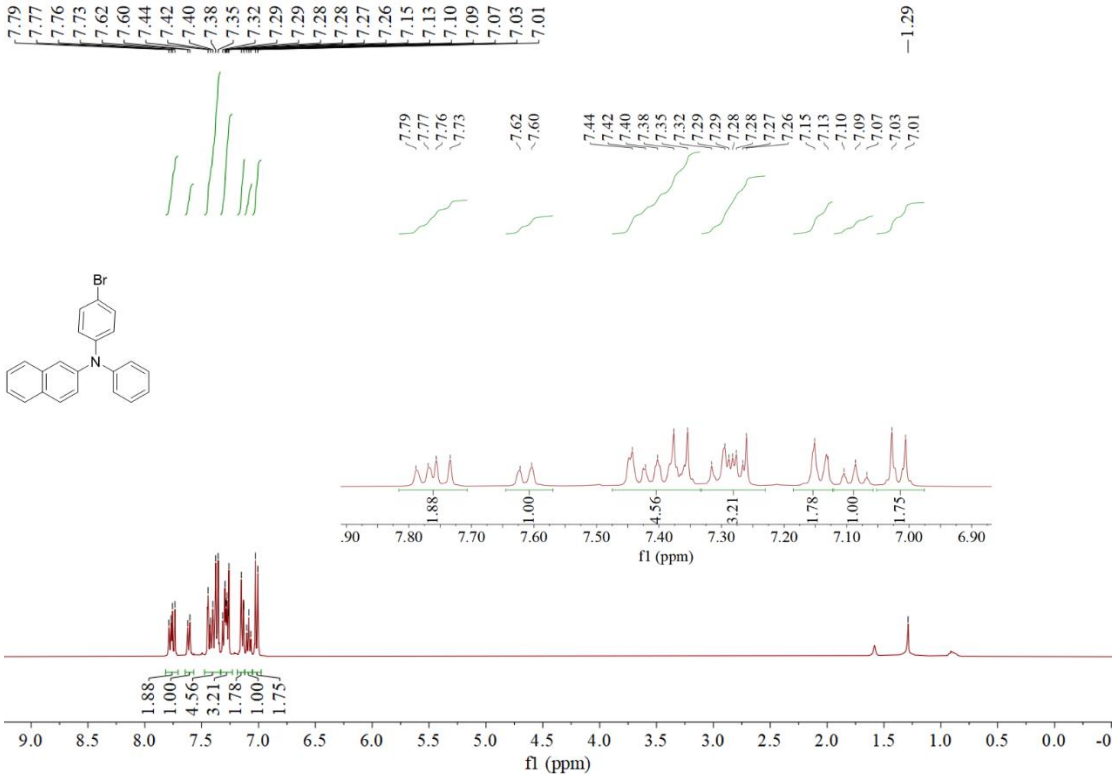

Figure S3. ^{1}H NMR spectrum of compound **βND-Br**.

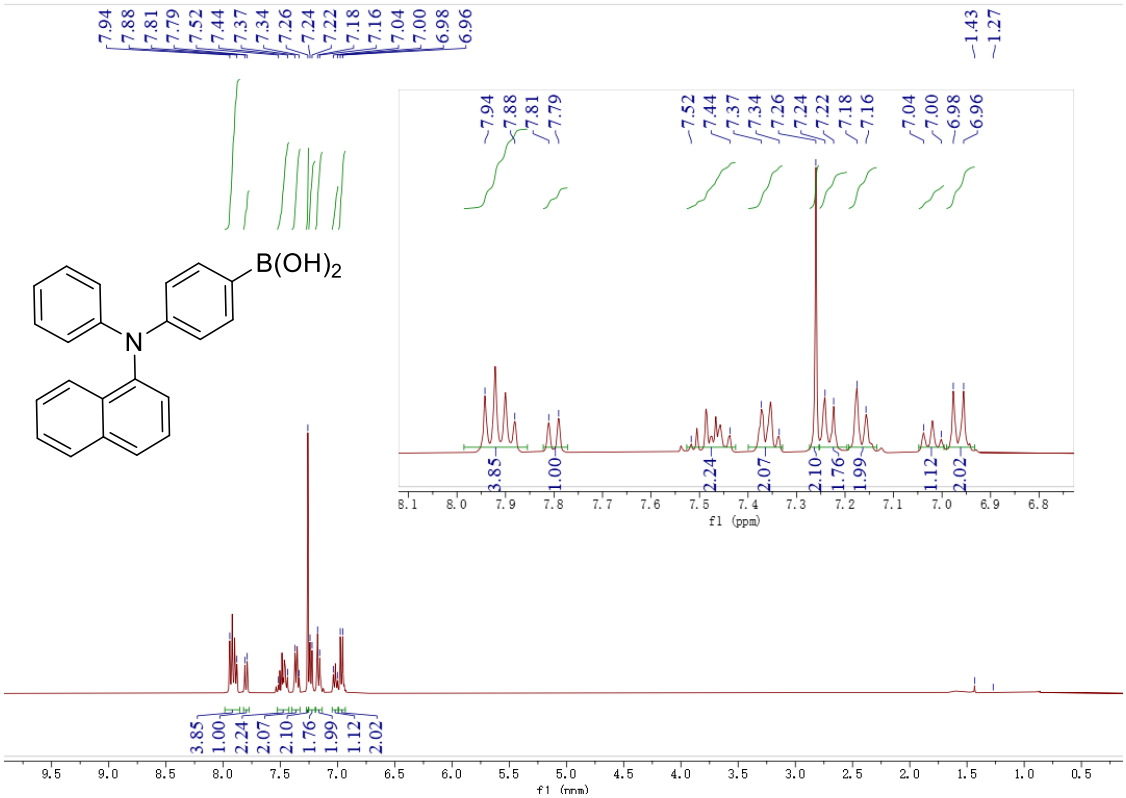

Figure S4. ^{1}H NMR spectrum of compound **αND-B(OH)$_2$**.

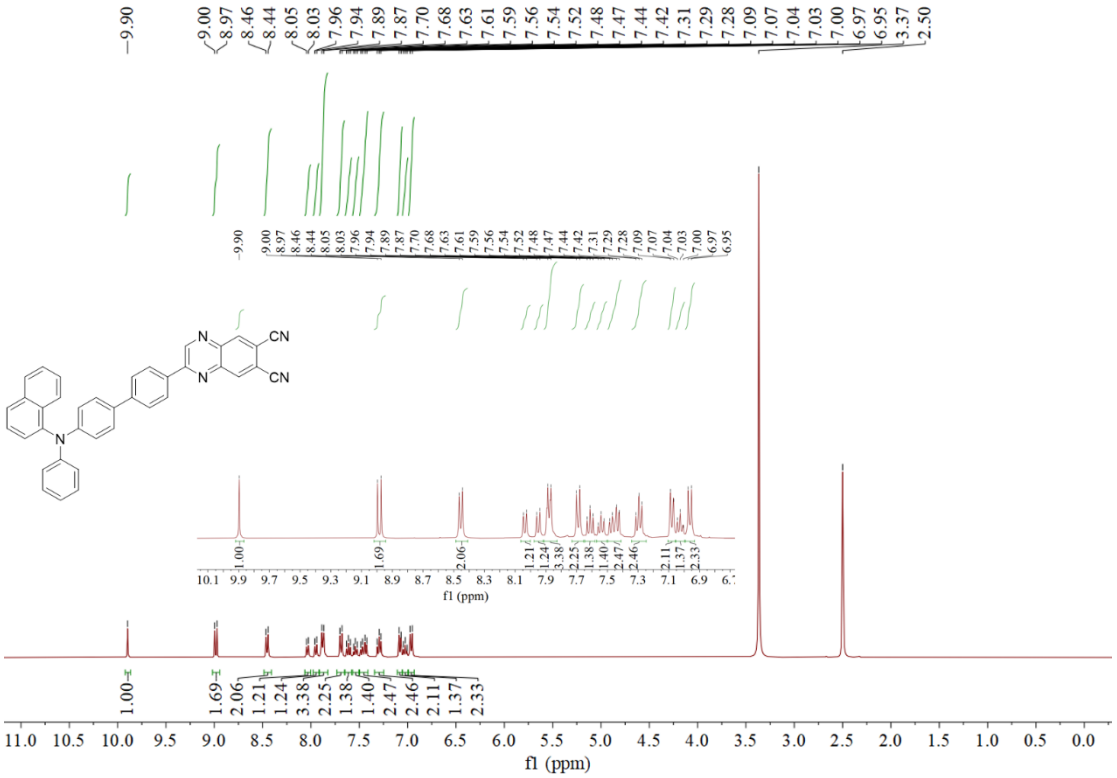

Figure S5. ^{1}H NMR spectrum of compound **αND-QCN**.

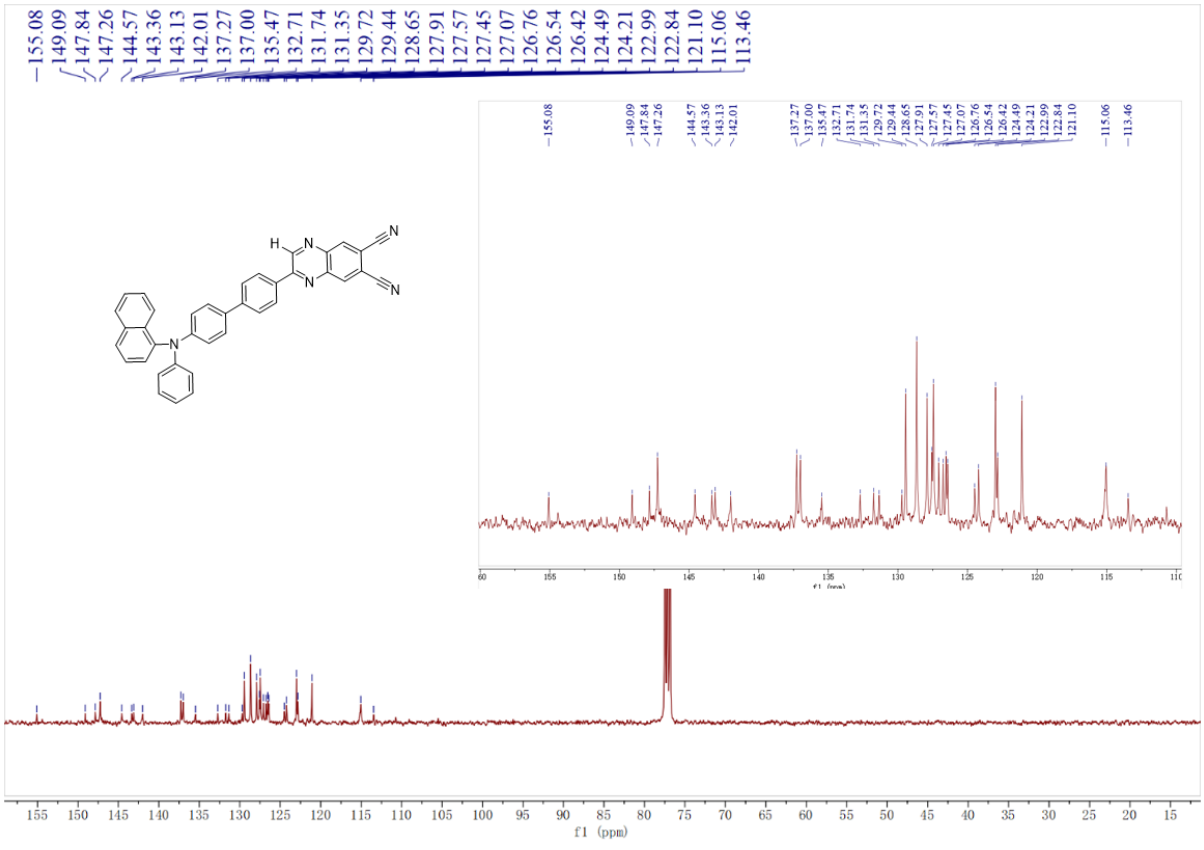

Figure S6. ^{13}C{^{1}H} NMR spectrum of compound **αND-QCN**.

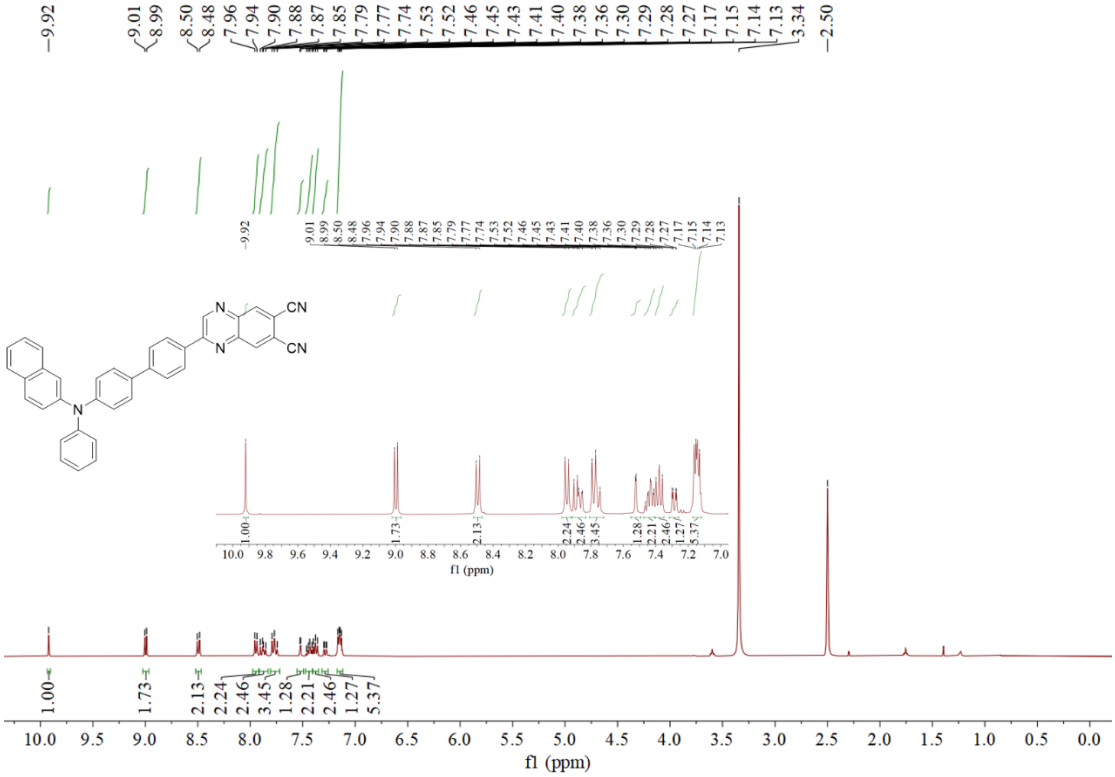

Figure S7. ^{1}H NMR spectrum of compound **βND-QCN**.

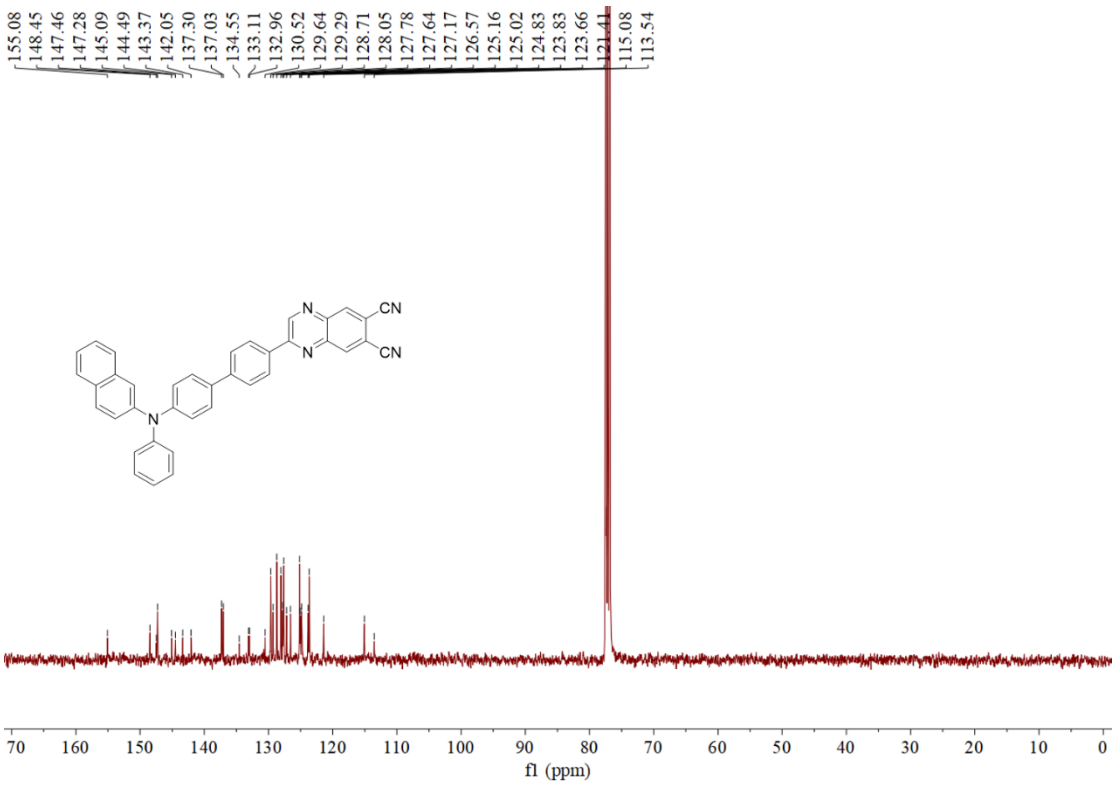

Figure S8. ^{13}C{^{1}H} NMR spectrum of compound **βND-QCN**.

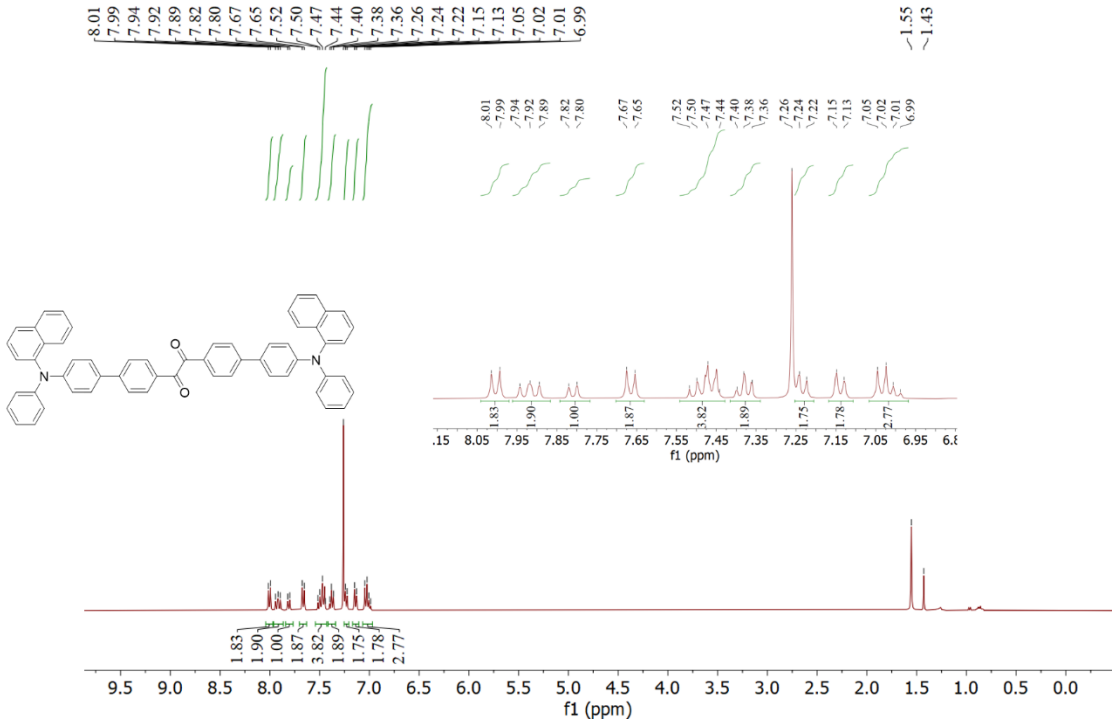

Figure S9. ^{1}H NMR spectrum of compound **(αND)$_2$-1,2-dione**.

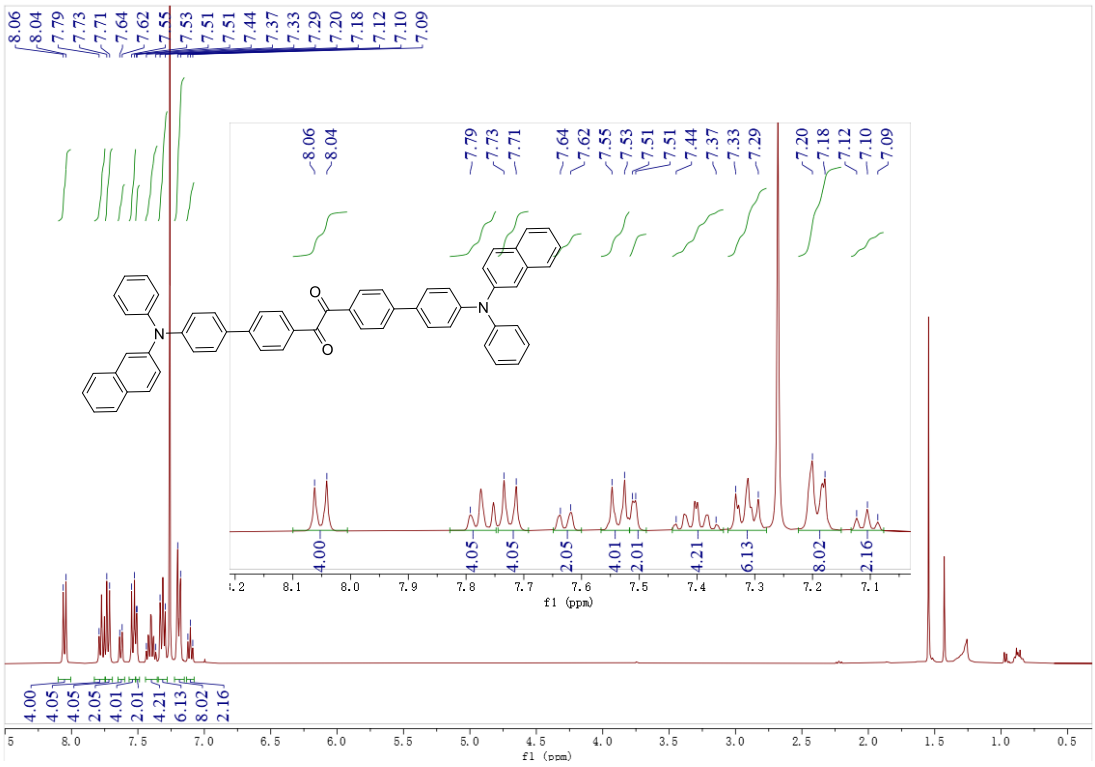

Figure S10. ^{1}H NMR spectrum of compound **(βND)$_2$-1,2-dione**.

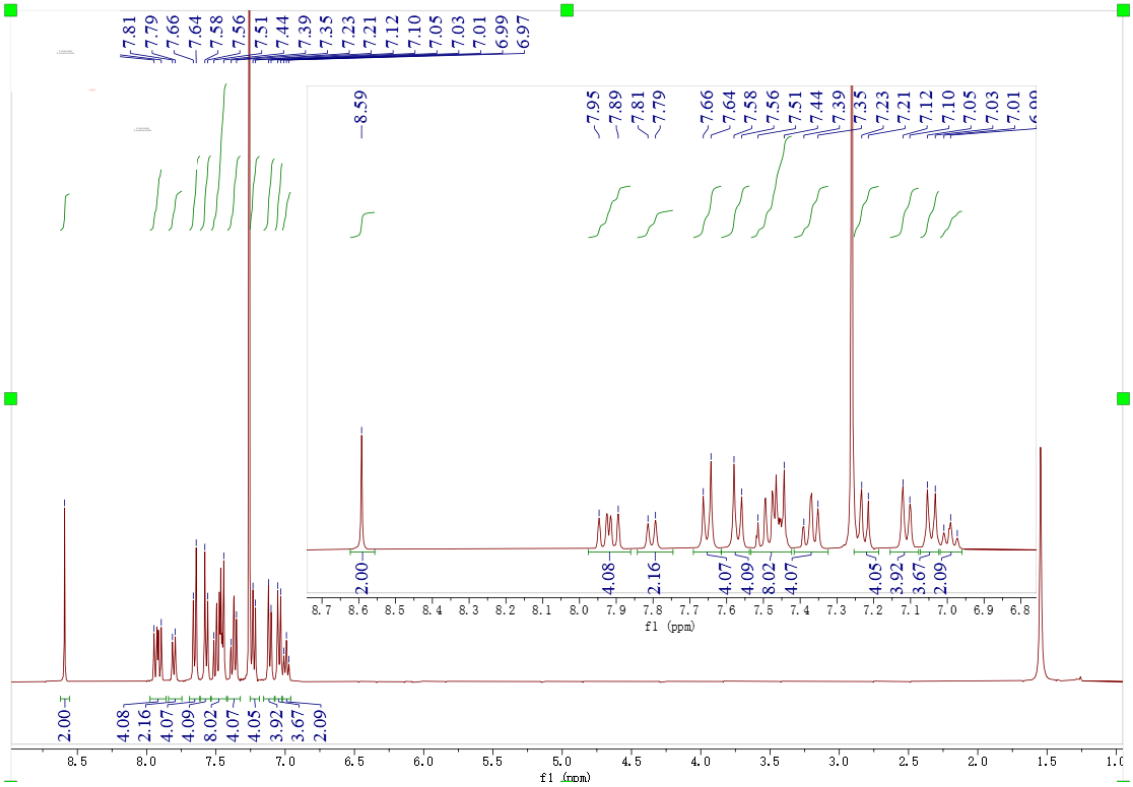

Figure S11. ^{1}H NMR spectrum of compound **(αND)$_2$-QCN**.

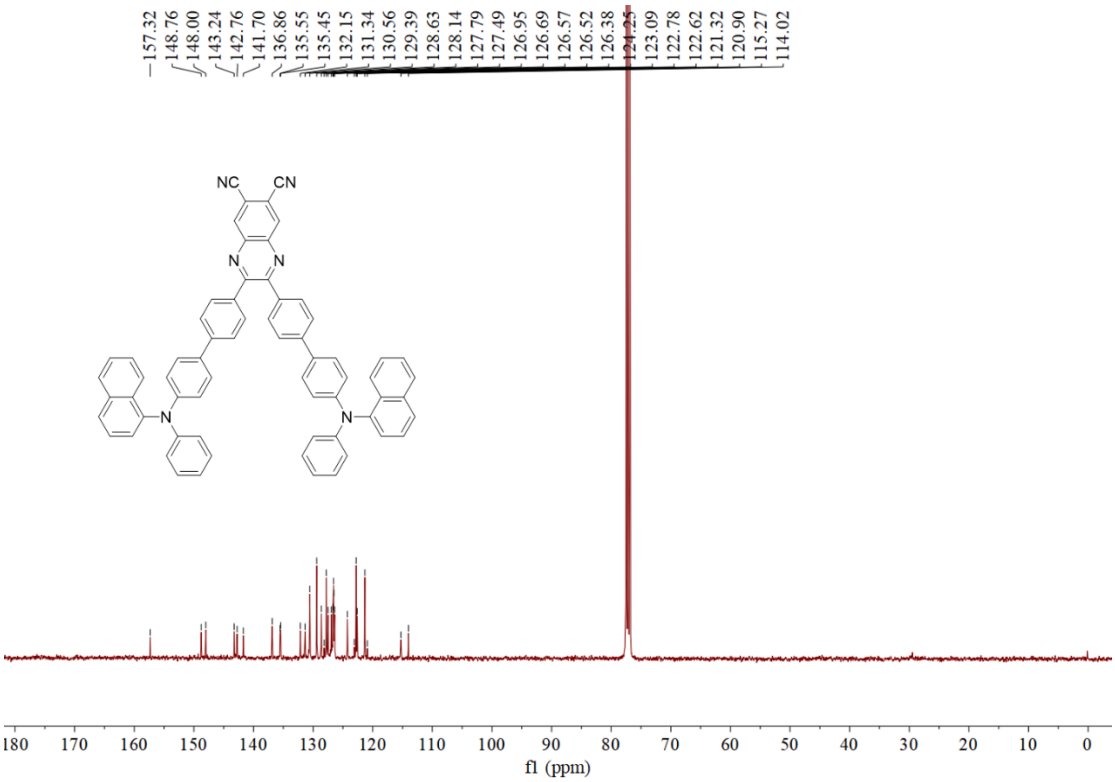

Figure S12. ^{13}C{^{1}H} NMR spectrum of compound **(αND)$_2$-QCN**.

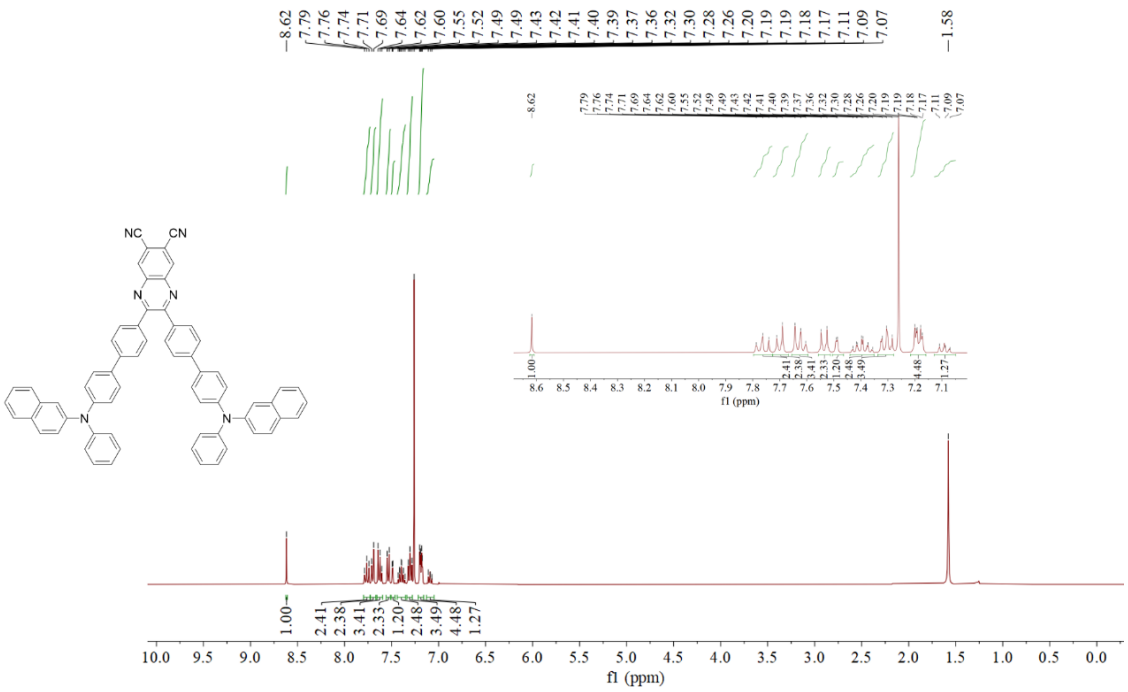

Figure S13. ^{1}H NMR spectrum of compound **(βND)$_2$-QCN**.

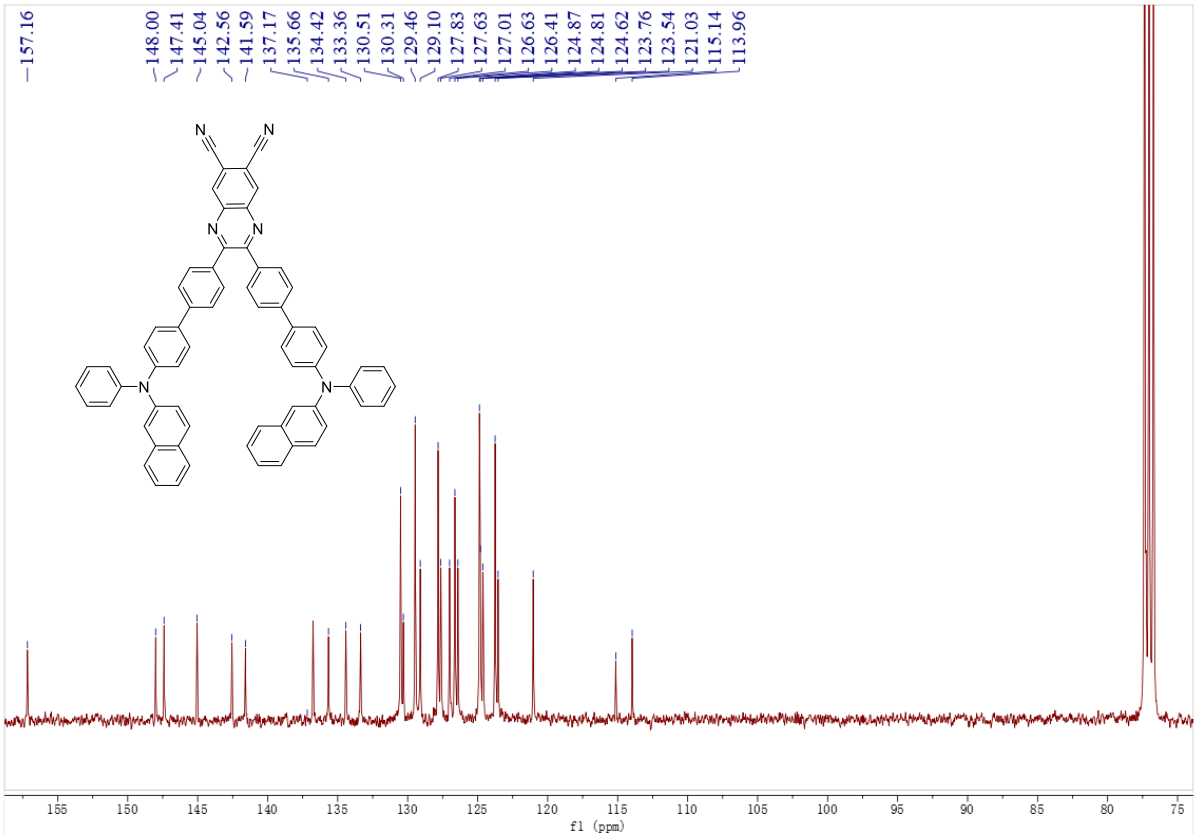

Figure S14. ^{13}C{^{1}H} NMR spectrum of compound **(βND)$_2$-QCN**.

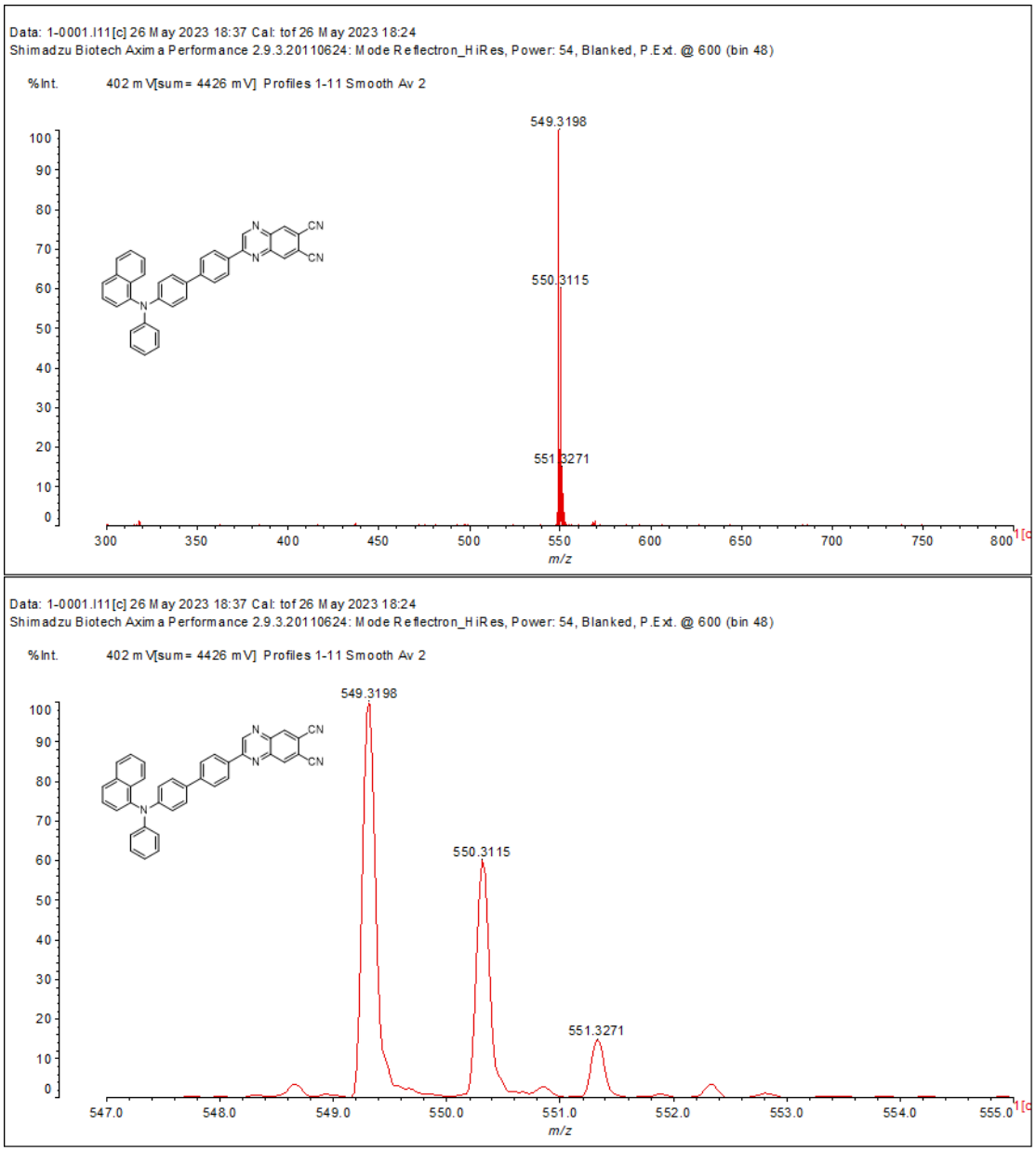

Figure S15. MALDI-TOF mass spectrometry of compound **αND-QCN**.

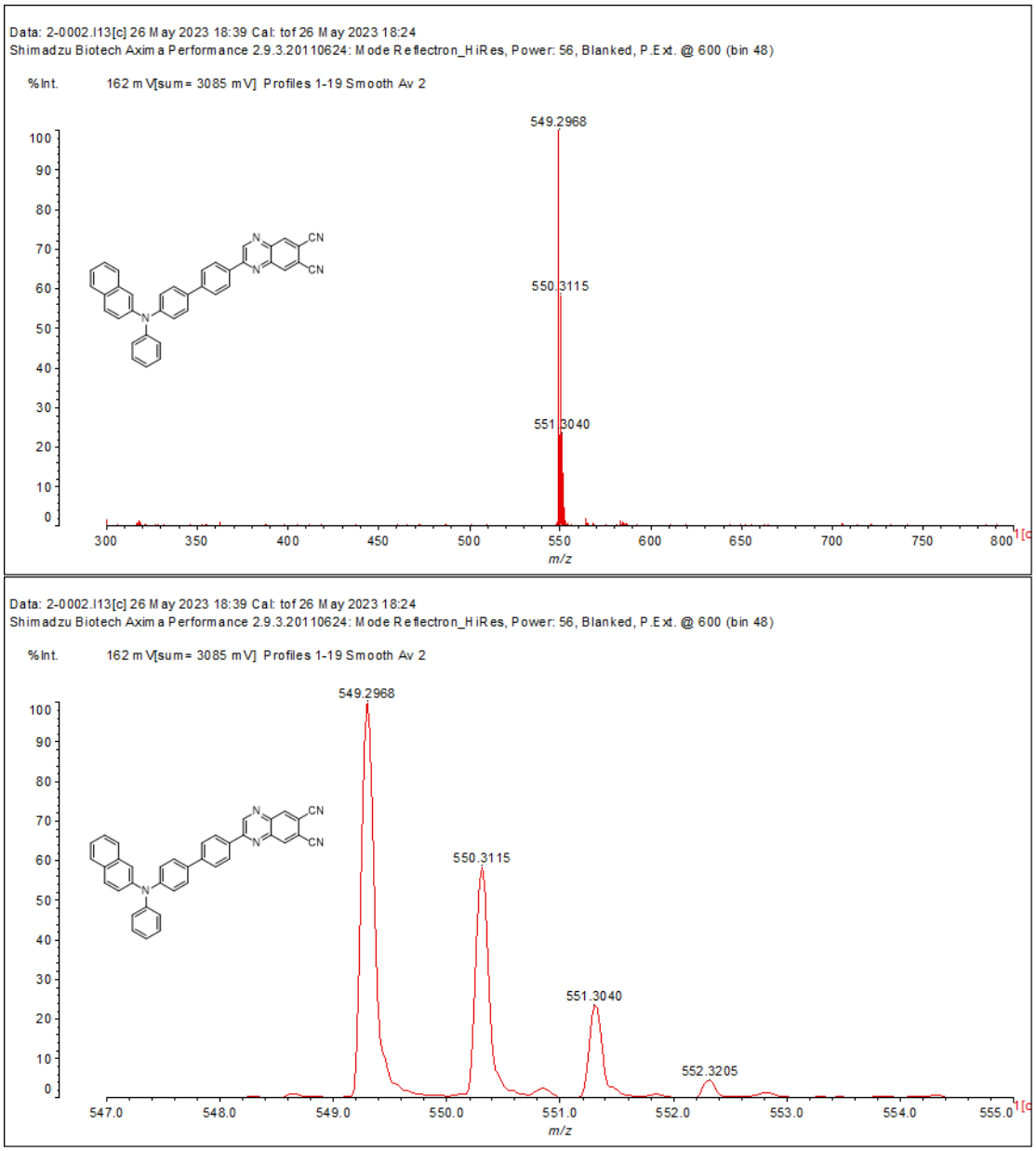

Figure S16. MALDI-TOF mass spectrometry of compound **βND-QCN**.

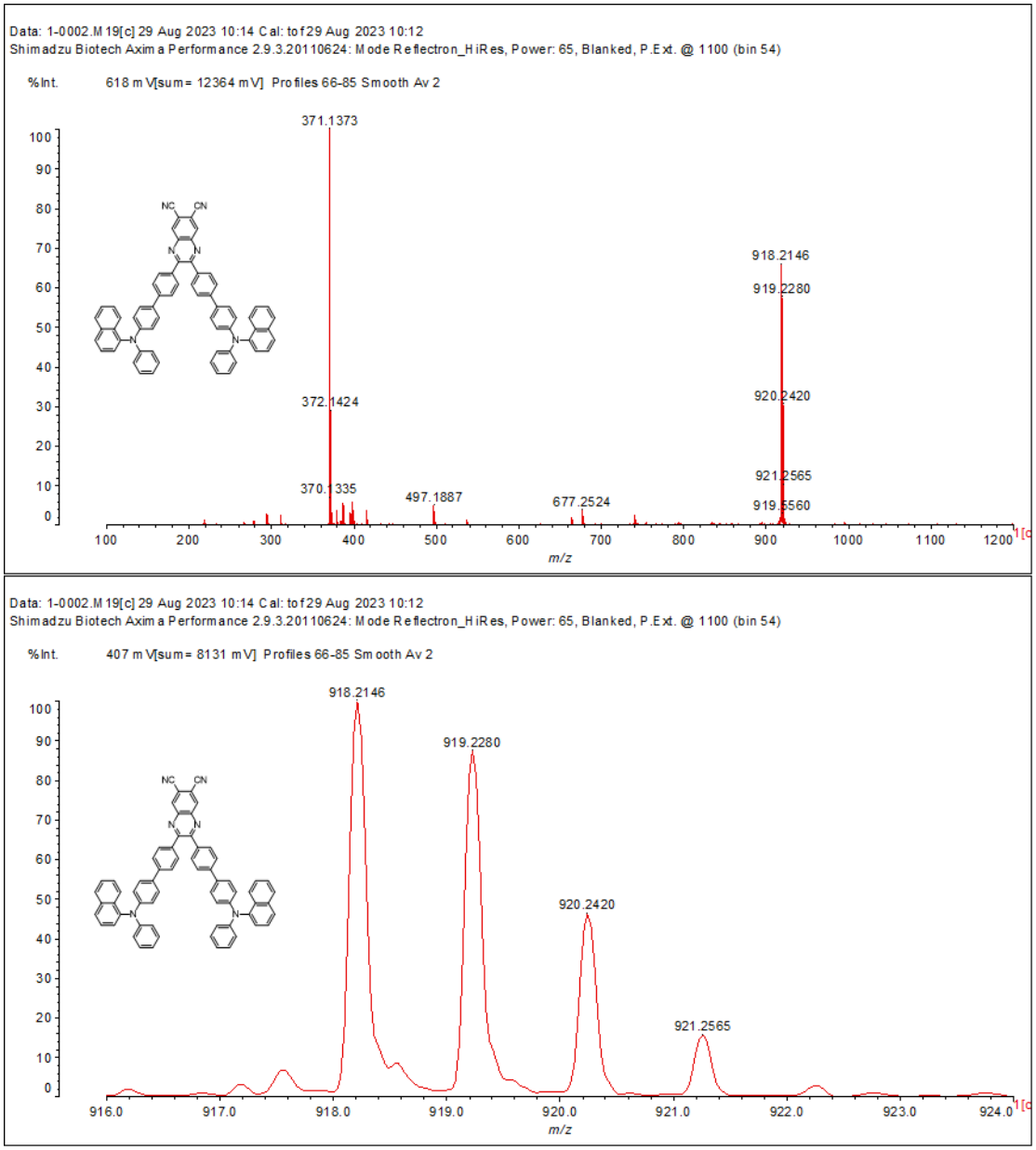

Figure S17. MALDI-TOF mass spectrometry of compound (**αND**)$_2$**-QCN**.

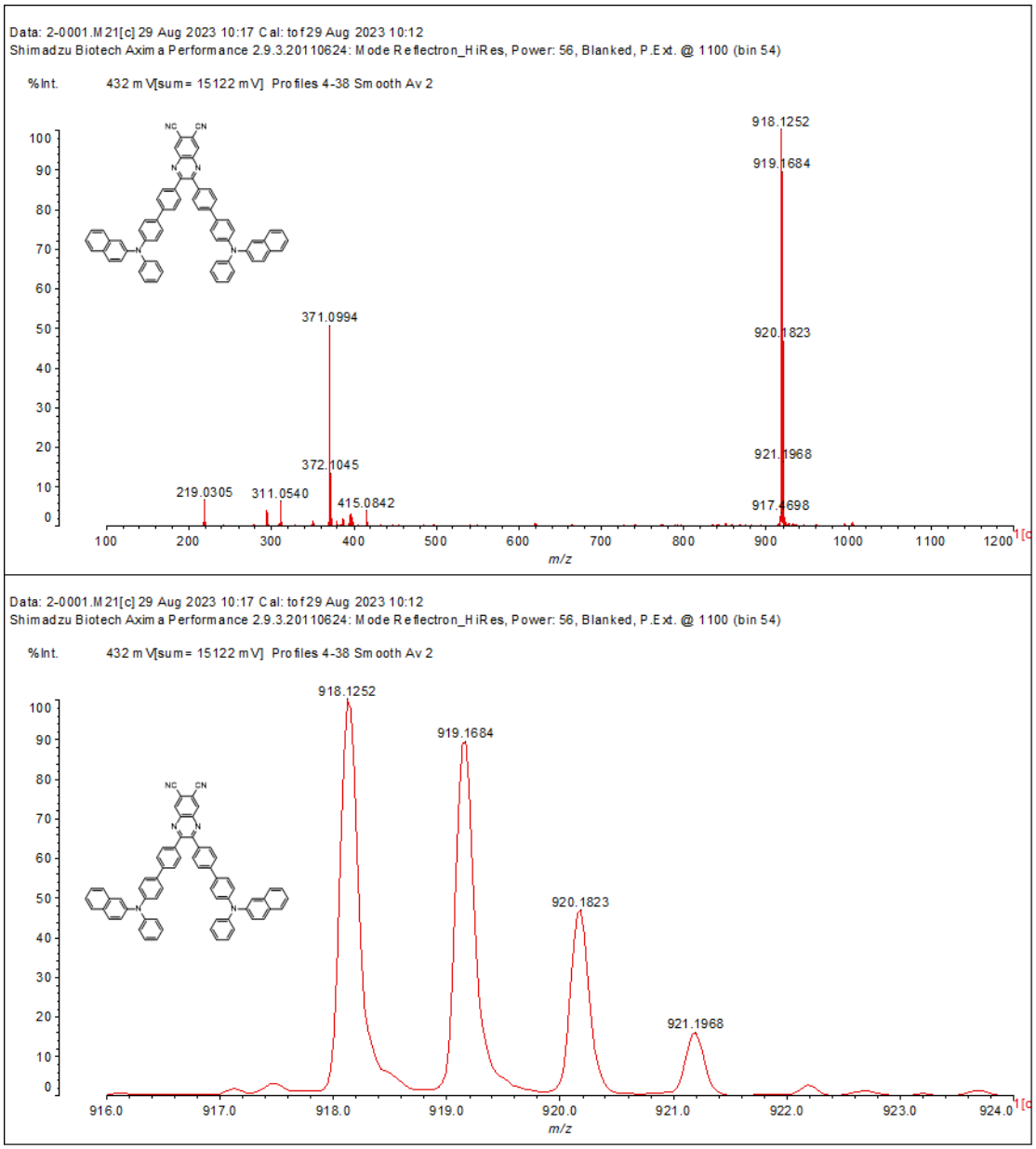

Figure S18. MALDI-TOF mass spectrometry of compound **(βND)$_2$-QCN**.

3. X-Ray Crystallography and Single-Crystal Structures

The single crystals suitable for structural elucidation by X-ray diffraction analysis were grown by slow diffusion of methanol vapors into a saturated chloroform solution of the corresponding compound. Suitable single crystals of compounds (plates) were selected under oil under ambient conditions and attached to the tip of a MiTeGenMicroMount©. Single crystal X-ray diffraction intensity data were collected in a stream of cold nitrogen at 180 K on a Bruker Quazar SMART APEXII diffractometer with Mo K_α (λ = 0.71073 Å) radiation. The intensity data was integrated using SAINT and corrected for absorption using SADABS routines.[4] The structures were solved by direct methods and refined by full-matrix least-squares on F^2 with anisotropic displacement parameters for the non-H hydrogen atoms using SHELXL-2013. [5]

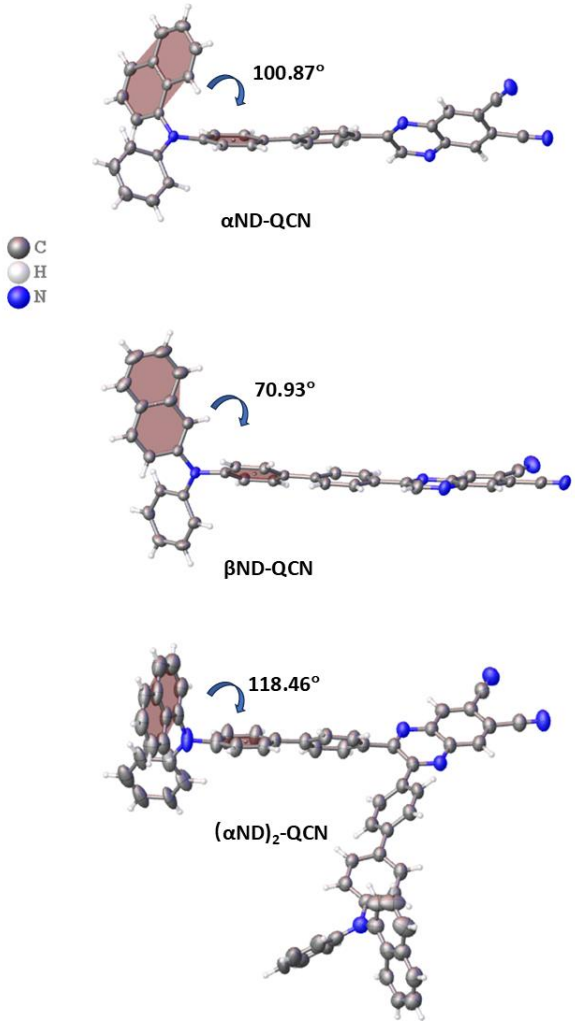

Figure S19. Single crystal structures of **αND-QCN**, **βND-QCN**, **(αND)$_2$-QCN** and their plane twist angles between naphthalene unit and phenyl group in naphthalene-substituted *N*,*N*-diphenylamine.

Table S1. Single crystal data for the molecule **αND-QCN**.

CCDC No.	2330756
Empirical formula	$C_{38}H_{23}N_5$
Formula weight	549.64
Temperature/K	180
Crystal system	monoclinic
Space group	P21/c
a/Å	22.3617(11)
b/Å	10.6853(4)
c/Å	11.8757(5)
α/°	90
β/°	99.540(4)
γ/°	90
Volume/Å³	2798.4(2)
Z	4
μ(mm^{-1})	0.079
F(000)	1144.0
D_x, (g cm^{-3})	1.305
Crystal size/mm^3	0.21×0.15×0.02
Radiation	Mo Kα (λ = 0.7103)
2Θ range for data collection/°	1.847 to 30.794
Index ranges	$-29 \leq h \leq 29$, $-13 \leq k \leq 13$, $-15 \leq l \leq 15$
Reflections collected	9253
Independent reflections	6789
Data completeness	1.056
Data/restraints/parameters	6789/0/389
Goodness-of-fit on F	1.044
Final R indexes [$I \geq 2\delta$ (I)]	R_1 = 0.0712, wR_2 = 0.1437
Final R indexes [all data]	R_1 = 0.1000, wR_2 = 0.1556

Table S2. Single crystal data for the molecule **βND-QCN**.

CCDC No.	2329072
Empirical	$C_{38}H_{23}N_5$
Formula weight	549.64
Temperature/K	180
Crystal system	orthorhombic
Space group	Pnc2
a/Å	8.1689(2)
b/Å	36.9002(9)
c/Å	9.8982(3)
α/°	90
β/°	90
γ/°	90
Volume/Å³	2983.66(14)
Z	4
μ (mm^{-1})	0.079
F(000)	1200.0
D_x, (g cm^{-3})	1.281
Crystal size/mm³	0.34×0.18×0.02
Radiation	Mo Kα (λ = 0.7103)
2Θ range for data collection/°	2.130 to 29.641
Index ranges	$-10 \leq h \leq 11$, $-51 \leq k \leq 44$, $-13 \leq l \leq 12$
Reflections collected	7621
Independent reflections	6586
Data completeness	1.71
Data/restraints/parameters	6586/3/417
Goodness-of-fit on F	1.073
Final R indexes [I ≥ 2δ (I)]	$R_1 = 0.0641$, $wR_2 = 0.1756$
Final R indexes [all data]	$R_1 = 0.0736$, $wR_2 = 0.1817$

Table S3. Single crystal data for the molecule **(αND)$_2$-QCN**.

CCDC No.	2339197
Empirical	$C_{66}H_{42}N_6$
Formula weight	919.10
Temperature/K	180
Crystal system	monoclinic
Space group	P 2n
a/Å	24.9637(8)
b/Å	8.0804(3)
c/Å	31.0995(13)
α/°	90
β/°	113.360(4)
γ/°	90
Volume/Å^3	5759.1(4)
Z	4
μ (mm^{-1})	0.063
F(000)	1920.0
D_x, (g cm^{-3})	1.060
Crystal size/mm^3	0.15×0.11×0.03
Radiation	Mo Kα (λ = 0.7103)
2Θ range for data collection/°	1.766 to 24. 410
Index ranges	$-29 \le h \le 29$, $-9 \le k \le 9$, $-37 \le l \le 36$
Reflections collected	10180
Independent reflections	5782
Data completeness	0.999
Data/restraints/parameters	5782/48/629
Goodness-of-fit on F	1.054
Final R indexes [I ≥ 2δ (I)]	R_1 = 0.0737, wR_2 = 0.1437
Final R indexes [all data]	R_1 = 0.1242, wR_2 = 0.2211

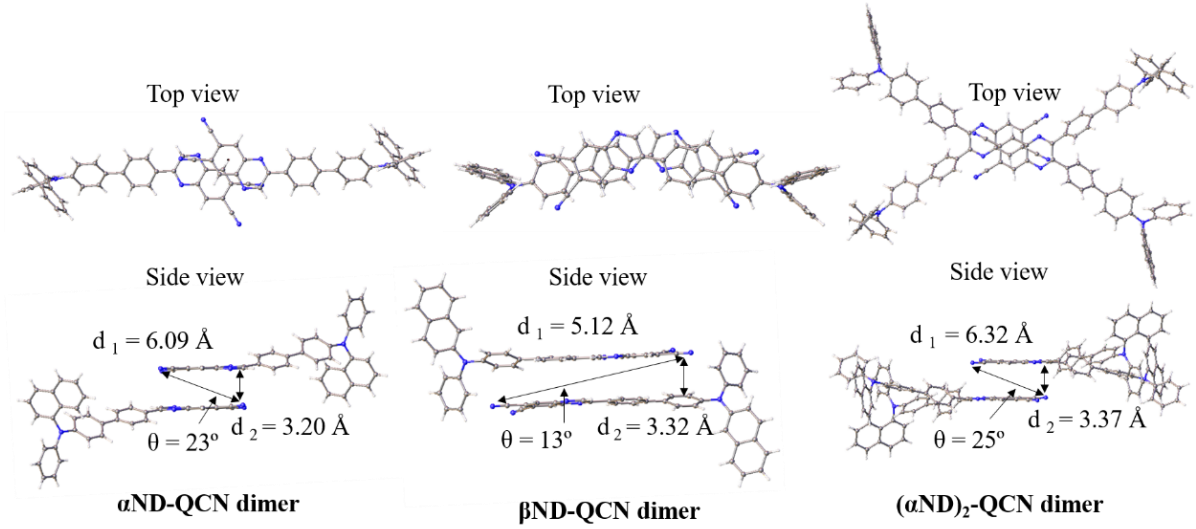

Figure S20. Single crystal structures of **αND-QCN**, **βND-QCN**, **(αND)$_2$-QCN** and their dimers in J-aggregates.

4. Thermal Properties

Thermogravimetric analyses (TGA) and differential scanning calorimetric (DSC) measurements were performed on TA Q50 and TA Q20, respectively. The heating rate is 10 °C min^{-1} from 40°C to 800 °C under nitrogen.

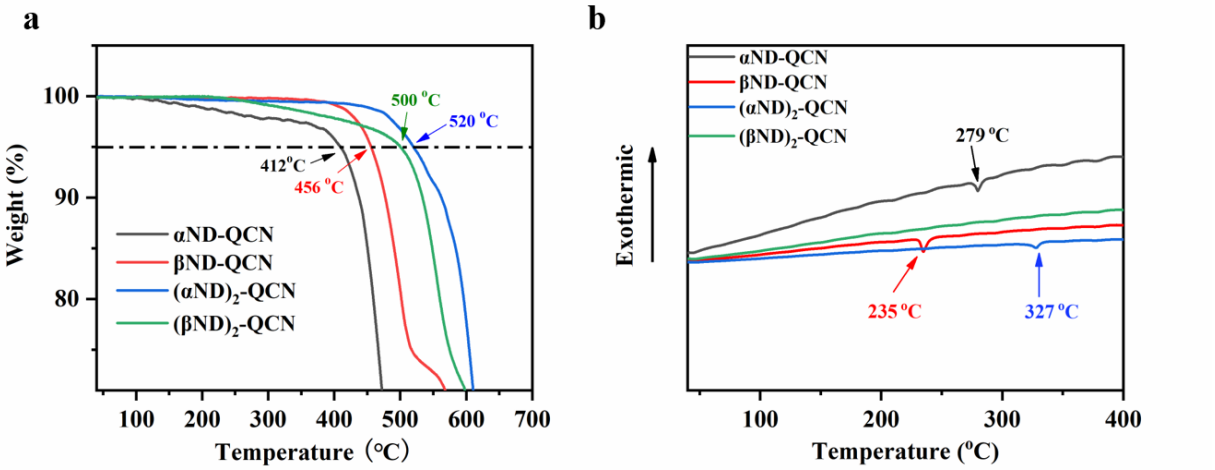

Figure S21. The TGA (a) and DSC (b) graphs of **αND-QCN**, **βND-QCN**, **(αND)$_2$-QCN** and **(βND)$_2$-QCN**.

5. Photophysical Properties

Spectroscopic grade solvents were used for recording UV-vis absorption and emission spectra. UV-vis absorption spectra were recorded on a Shimadzu UV-3600 spectrophotometer. The emission spectra, absolute fluorescence quantum yields, and fluorescence decay lifetime of compounds in solutions, doped films (30 wt.% doped in TPBi), and solid powder were measured on an Edinburgh FLS980 fluorimeter. Phosphorescence spectra can be measured using gating spectra by setting delay times at different times controlled on the Edinburgh FLS980 fluorimeter. The ΔE_{ST} (S_1-T_1) is determined by the fluorescence and phosphorescence spectra at 77 K, in which the energy of S_1 can be calculated from the onset of the fluorescence spectrum, and the phosphorescence spectrum at 77 K clearly indicates the T_1 which can be derived from the $E_{0\text{-}0}$ band. [6-8]

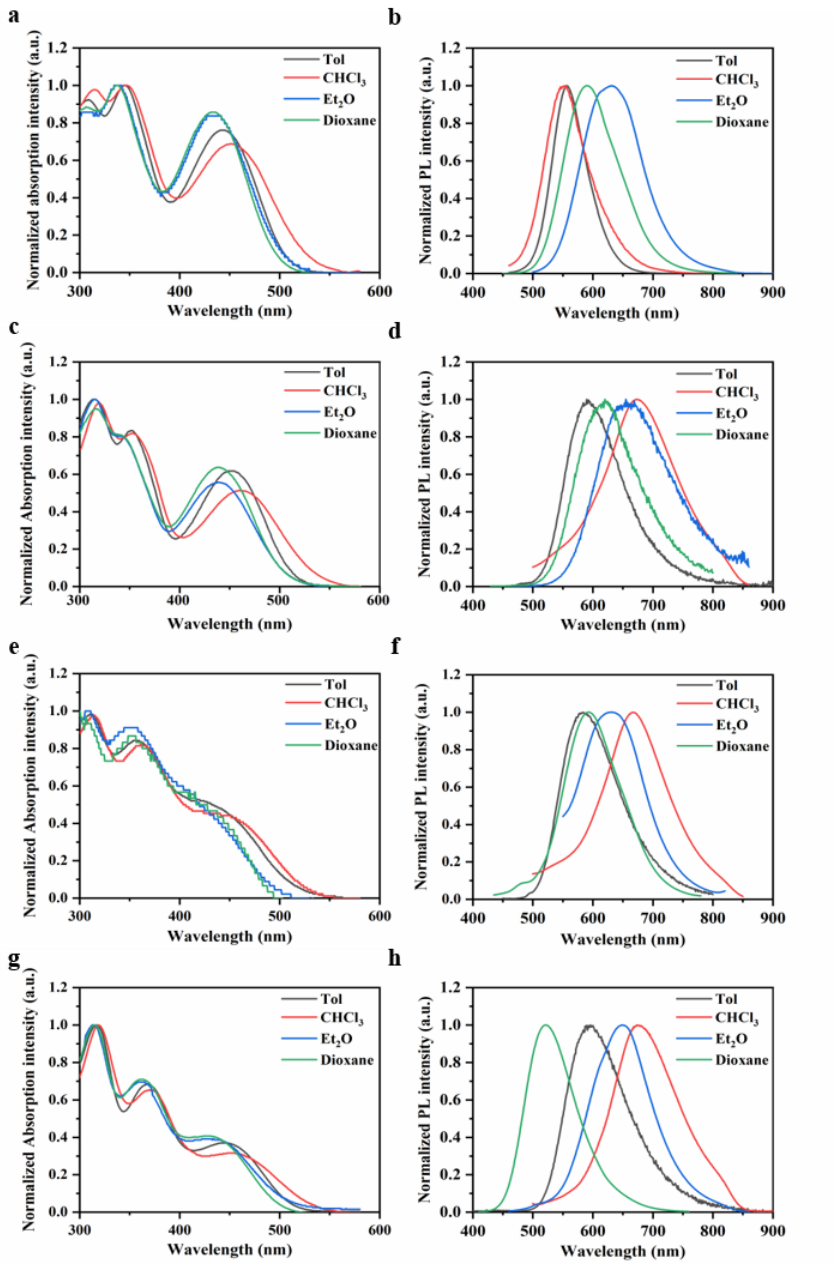

Figure S22. UV-vis absorption spectra and photoluminescence spectra of **αND-QCN** (a, b), **βND-QCN** (c, d), **(αND)$_2$-QCN** (e, f), **(βND)$_2$-QCN** (g, h) in different solvents (10^{-5} M) at room temperature; Excitation wavelengths for **αND-QCN**, **βND-QCN**, **(αND)$_2$-QCN** and **(βND)$_2$-QCN** in dioxane/Et_2O/Tol/$CHCl_3$ are 430/460/440/440 nm, 440/440/450/460 nm, 400/420/488/460 nm, and 440/480/470/480 nm, respectively.

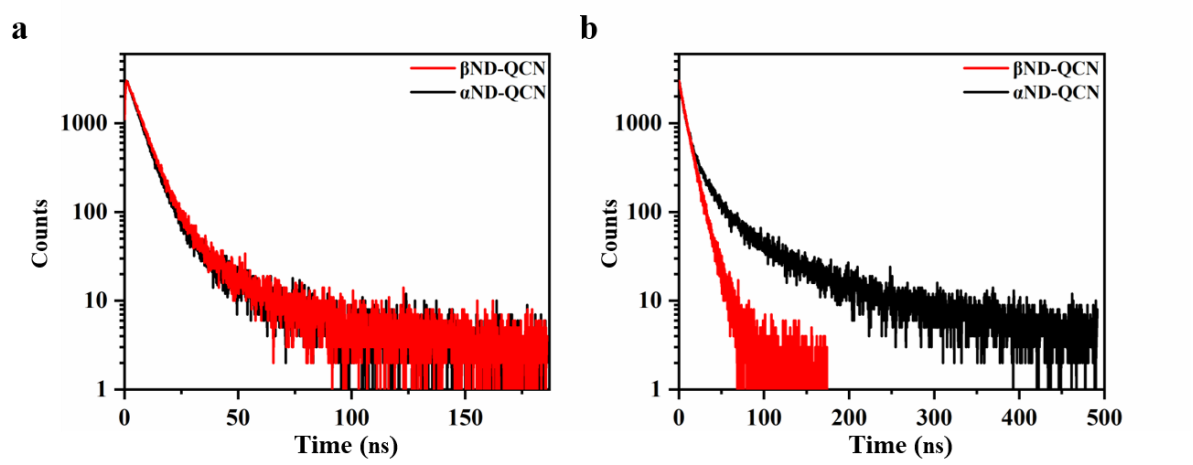

Figure S23. The transient fluorescence decay spectra of **αND-QCN** and **βND-QCN** in toluene (10^{-5} M) (a) and solid powder (b).

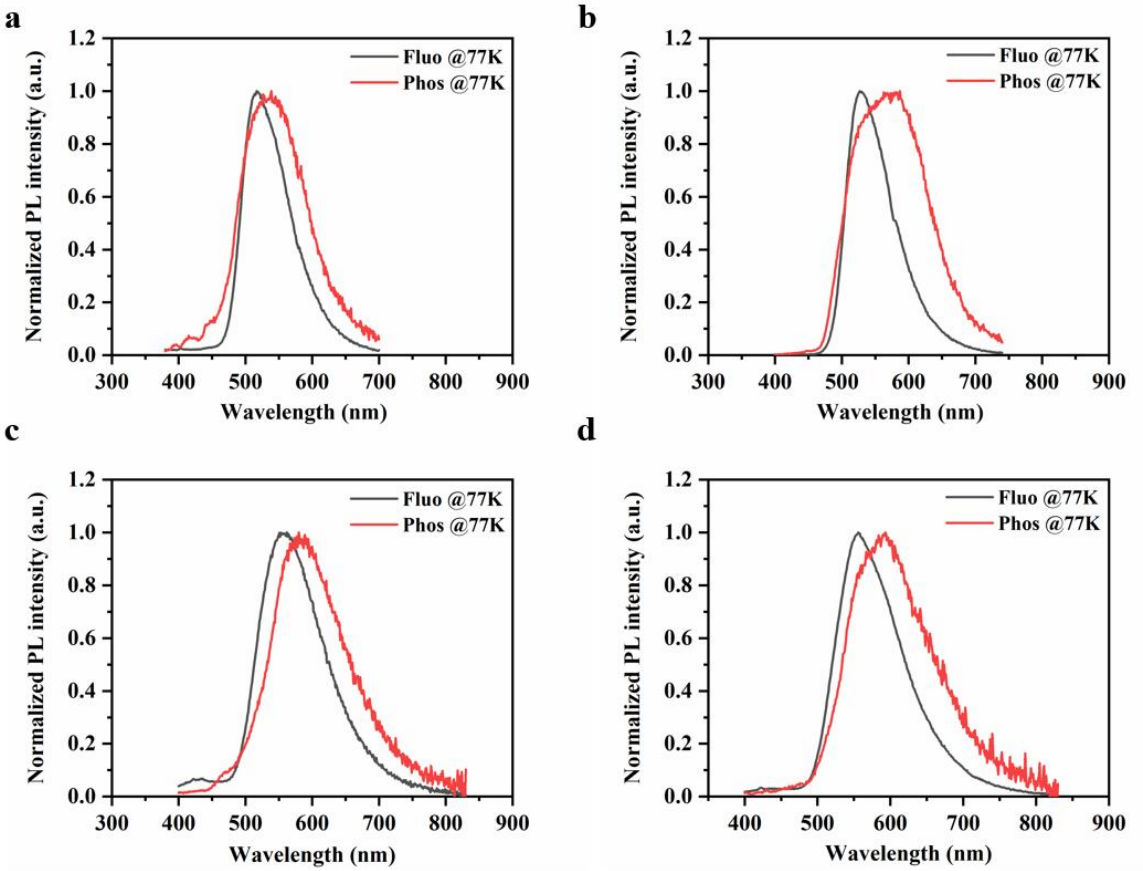

Figure S24. Fluorescence and phosphorescence spectra of **αND-QCN** (a), **βND-QCN** (b), **(αND)$_2$-QCN** (c) and **(βND)$_2$-QCN** (d) measured in toluene solution (1.0×10^{-5} M) at 77 K. Excitation wavelengths for **αND-QCN**, **βND-QCN**, **(αND)$_2$-QCN** and **(βND)$_2$-QCN** are 440 nm, 450 nm, 420 nm and 440 nm, respectively.

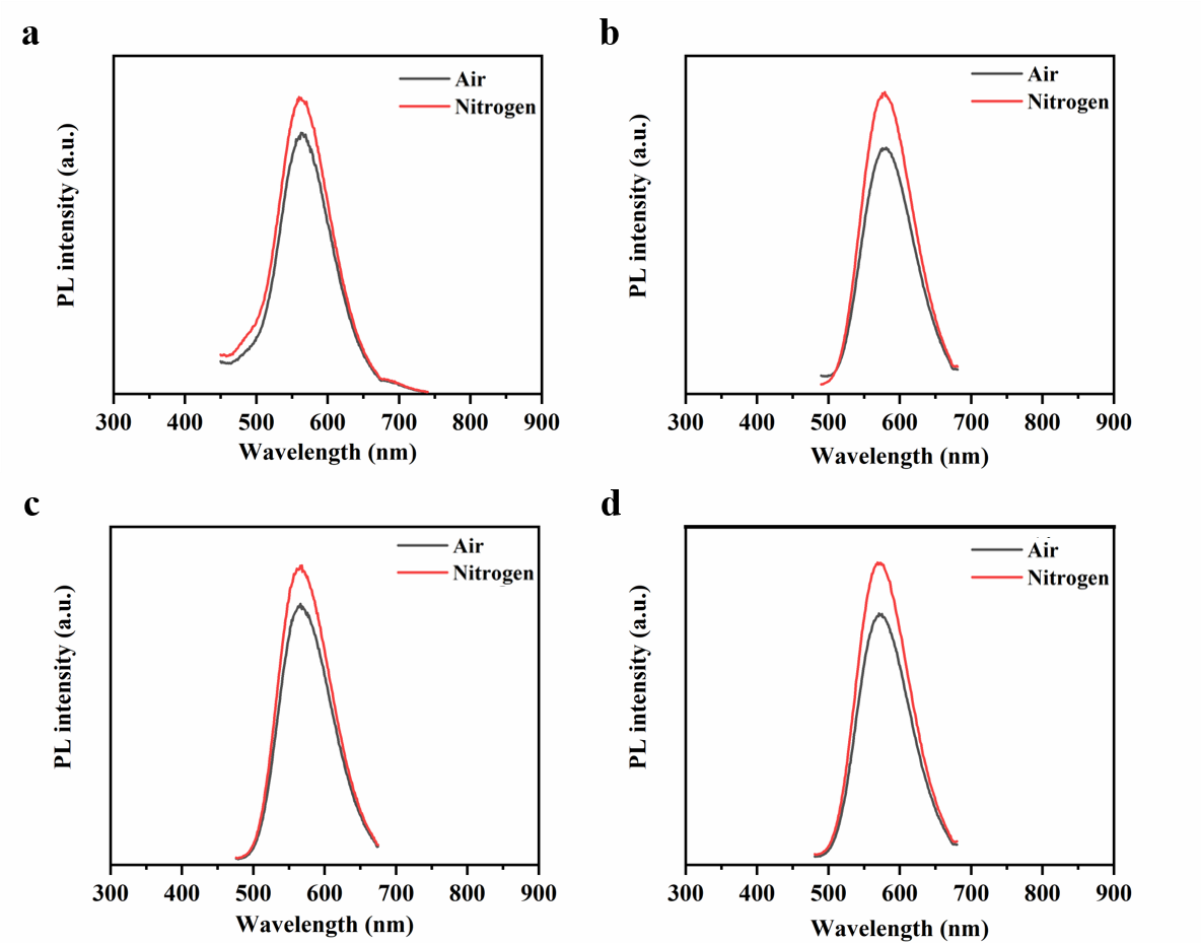

Figure S25. The PL spectra of **αND-QCN** (a), **βND-QCN** (b), **(αND)$_2$-QCN** (c) and **(βND)$_2$-QCN** (d) in toluene solution (10^{-5} M) recorded at room temperature under air and nitrogen atmospheres. Excitation wavelengths for **αND-QCN**, **βND-QCN**, **(αND)$_2$-QCN** and **(βND)$_2$-QCN** are 440 nm, 450 nm, 420 nm and 440 nm, respectively.

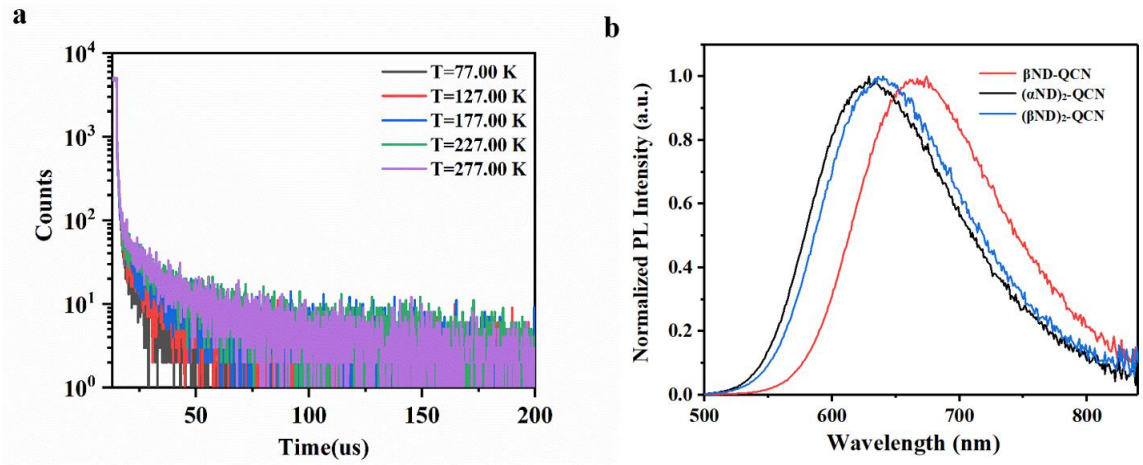

Figure S26. (a) Temperature-dependent transient PL decay of **βND-QCN** in doped film; (b) Photoluminescence spectra of **βND-QCN**, **(αND)$_2$-QCN** and **(βND)$_2$-QCN** in thermally evaporated doped films (30 wt.% doped in TPBi).

6. Theoretical Calculations

Geometry optimizations, HOMO/LUMO, excited states, ONIOM 2-layer calculations B3LYP/6-31G(d):UFF (UFF=Universal Force Field) calculations,[9] and Natural Transitional Orbital (NTO) analysis [10] were performed at the TD-DFT level of theory /DFT level of theory, respectively, using B3LYP functional [11] and 6-31G (d) basis set [12] as implemented in the Gaussian 09 package.[13]

Table S4. Cartesian coordinates of the optimized ***α*ND-QCN** structure.

Center number	Atomic number	Coordinates		
		X	Y	Z
1	6	-1.35287	-0.72097	-0.89312
2	6	-2.74767	-0.70311	-1.02077
3	6	-3.49366	0.344659	-0.44567
4	6	-2.83722	1.370962	0.251854
5	6	-1.4421	1.35231	0.37897
6	6	-0.69992	0.305743	-0.19193
7	1	-0.77699	-1.4925	-1.36972
8	1	-3.24513	-1.45884	-1.5997
9	1	-3.41186	2.143701	0.726426
10	1	-0.94338	2.108951	0.956181
11	6	-5.02396	0.361159	-0.59276
12	6	-5.6026	1.098942	-1.64759
13	1	-4.96043	1.609997	-2.36244
14	6	-7.14554	-0.26258	0.143226
15	6	-7.72888	0.470318	-0.9286
16	6	-7.98617	-0.91713	1.088796
17	6	-9.14605	0.498501	-1.07393
18	6	-9.38055	-0.87225	0.933107
19	1	-7.56833	-1.45443	1.920849
20	6	-9.95779	-0.17006	-0.14454
21	1	-9.60761	1.027275	-1.88834
22	7	-5.80254	-0.34314	0.249718
23	7	-6.93857	1.128418	-1.8038
24	6	-10.2763	-1.58532	1.921922
25	6	-11.4632	-0.14289	-0.29164

26	7	-10.9565	-2.1297	2.676255
27	7	-12.6094	-0.11792	-0.4098
28	6	0.816742	0.286782	-0.05107
29	6	1.616094	0.983775	-0.9682
30	6	1.415252	-0.42689	0.995746
31	6	3.011761	0.951456	-0.85365
32	1	1.156932	1.517274	-1.7786
33	6	2.808915	-0.42362	1.133529
34	1	0.802759	-0.93735	1.714841
35	6	3.621927	0.238636	0.194391
36	1	3.602876	1.47318	-1.56906
37	1	3.265838	-0.9374	1.959211
38	7	5.079123	0.160943	0.434606
39	6	5.571203	1.538832	0.606758
40	6	6.213239	2.243331	-0.4348
41	6	5.390439	2.161001	1.850748
42	6	6.661707	3.557485	-0.22722
43	1	6.360065	1.780367	-1.39115
44	6	5.836537	3.475699	2.056047
45	1	4.900914	1.628161	2.640115
46	6	6.475588	4.174848	1.019305
47	1	7.150551	4.088497	-1.02097
48	1	5.690826	3.944501	3.009033
49	1	6.818025	5.178847	1.179632
50	6	5.892701	-0.60731	-0.55127
51	6	6.869713	-1.45269	0.02439
52	6	5.775337	-0.57011	-1.95627
53	6	7.711102	-2.25196	-0.79634
54	6	7.0084	-1.51858	1.431749
55	6	6.610447	-1.35822	-2.7674
56	1	5.057712	0.053178	-2.42576
57	6	7.576383	-2.19455	-2.19639
58	6	8.675691	-3.09591	-0.20235
59	6	7.970269	-2.3614	2.008233
60	1	6.374783	-0.92449	2.065719
61	1	6.509588	-1.31425	-3.83434
62	1	8.205696	-2.79602	-2.82869

63	6	8.803086	-3.15002	1.192248
64	1	9.314904	-3.70293	-0.81948
65	1	8.07007	-2.40646	3.07617
66	1	9.53873	-3.79272	1.638063

Table S5. Cartesian coordinates of the optimized **βND-QCN** structure.

Center number	Atomic number	Coordinates		
		X	Y	Z
1	6	-1.41237	-0.32756	-1.17572
2	6	-2.81388	-0.35865	-1.2492
3	6	-3.5827	0.522746	-0.45368
4	6	-2.9407	1.432282	0.407962
5	6	-1.53926	1.463099	0.480987
6	6	-0.77881	0.58202	-0.3097
7	1	-0.82593	-0.95705	-1.80996
8	1	-3.29919	-1.00939	-1.94381
9	1	-3.52487	2.063509	1.040118
10	1	-1.05157	2.115291	1.173707
11	6	-5.13395	0.483719	-0.54328
12	6	-5.78186	1.373606	-1.41456
13	1	-5.18954	2.041017	-2.03964
14	6	-7.21752	-0.3906	0.140139
15	6	-7.8741	0.495468	-0.74814
16	6	-7.9912	-1.25645	0.974314
17	6	-9.30154	0.474585	-0.83778
18	6	-9.405	-1.26086	0.879171
19	1	-7.52019	-1.91668	1.673309
20	6	-10.0546	-0.4045	-0.02103
21	1	-9.82197	1.117935	-1.51749
22	7	-5.86738	-0.41065	0.173384
23	7	-7.13974	1.344302	-1.5034
24	6	-10.2468	-2.20966	1.757237
25	6	-11.5946	-0.43485	-0.1076
26	7	-10.872	-2.91438	2.409434
27	7	-12.7383	-0.45329	-0.17598
28	6	0.750625	0.616844	-0.22663

29	6	1.472738	1.520515	-1.02782
30	6	1.421321	-0.25939	0.646058
31	6	2.873847	1.538511	-0.96875
32	1	0.956864	2.162901	-1.70644
33	6	2.820269	-0.21132	0.73633
34	1	0.864342	-0.92507	1.268268
35	6	3.544079	0.675564	-0.09007
36	1	3.431776	2.191978	-1.6
37	1	3.335613	-0.84503	1.426501
38	7	5.004802	0.701414	-0.00441
39	6	5.447047	2.041307	0.396328
40	6	5.824619	2.972746	-0.59741
41	6	5.49482	2.399836	1.753994
42	6	6.245621	4.264656	-0.22966
43	1	5.786393	2.69804	-1.63202
44	6	5.91353	3.692885	2.1226
45	1	5.205628	1.695717	2.496718
46	6	6.292133	4.624004	1.132208
47	1	6.531918	4.967847	-0.97842
48	1	5.946358	3.965889	3.151681
49	1	6.610619	5.601603	1.414807
50	6	5.891469	-0.43879	-0.27766
51	6	5.823765	-1.0737	-1.54156
52	6	6.773251	-0.88421	0.676347
53	6	6.638671	-2.14101	-1.8268
54	1	5.109123	-0.69839	-2.28883
55	6	7.628974	-1.98733	0.407752
56	1	6.833462	-0.39759	1.661248
57	6	7.561545	-2.62371	-0.8586
58	1	6.593067	-2.64053	-2.80615
59	6	8.552091	-2.47077	1.375463
60	6	8.417598	-3.727	-1.12715
61	6	9.36725	-3.53795	1.090168
62	1	8.597959	-1.97151	2.354954
63	6	9.299577	-4.1727	-0.17403
64	1	8.357357	-4.21377	-2.11208
65	1	10.08204	-3.91306	1.837349

66	1	9.963131	-5.02582	-0.37843

Table S6. Cartesian coordinates of the optimized **(αND)$_2$-QCN** structure.

Center number	Atomic number	Coordinates X	Y	Z
1	6	3.855748	2.498537	0.336021
2	6	2.934718	3.523526	0.453924
3	6	1.629533	3.381667	-0.03589
4	6	1.293259	2.168876	-0.65796
5	6	2.227007	1.151388	-0.79042
6	6	3.529823	1.282548	-0.29079
7	1	4.847849	2.651676	0.746613
8	1	3.219137	4.452377	0.936027
9	1	0.306201	2.017598	-1.06915
10	1	1.92056	0.243175	-1.29785
11	6	0.724268	4.556933	0.067441
12	6	-0.74811	4.582483	-0.12614
13	6	0.693372	6.872319	0.12326
14	6	-0.67175	6.88275	-0.26114
15	6	1.377172	8.089962	0.315908
16	6	-1.33415	8.105934	-0.48423
17	6	0.717837	9.296922	0.121617
18	1	2.421895	8.070464	0.605975
19	6	-0.66534	9.305092	-0.28416
20	1	-2.37264	8.099926	-0.80219
21	7	1.345708	5.690699	0.279547
22	7	-1.34816	5.713206	-0.37893
23	6	1.424858	10.52787	0.327217
24	6	-1.36021	10.54423	-0.48358
25	7	2.010673	11.51796	0.498484
26	7	-1.93382	11.54652	-0.64607
27	6	4.523703	0.180916	-0.40613
28	6	4.188033	-1.06018	-0.98317
29	6	5.829121	0.323173	0.076111
30	6	5.064191	-2.13198	-0.95191
31	1	3.227577	-1.20271	-1.4661

32	6	6.714299	-0.74577	0.111092
33	1	6.180872	1.286191	0.431444
34	6	6.315394	-2.00708	-0.32719
35	1	4.777159	-3.0756	-1.40526
36	1	7.721852	-0.59254	0.485835
37	7	7.094822	-3.19642	-0.09715
38	6	7.369793	-3.9985	-1.27713
39	6	7.52554	-5.37741	-1.08493
40	6	7.416705	-3.48357	-2.57759
41	6	7.584051	-6.23954	-2.17883
42	1	7.595686	-5.7658	-0.07186
43	6	7.458415	-4.35029	-3.66946
44	1	7.409786	-2.40917	-2.73908
45	6	7.512697	-5.7304	-3.47789
46	1	7.67865	-7.31066	-2.01525
47	1	7.446916	-3.94175	-4.67759
48	1	7.494509	-6.40305	-4.33219
49	6	7.720478	-2.97725	2.194116
50	6	8.607304	-3.00327	3.292735
51	6	8.167213	-3.03341	0.878776
52	6	9.966038	-3.08401	3.065779
53	6	9.575718	-2.99079	0.609752
54	6	10.47258	-3.06669	1.735243
55	1	10.66657	-3.1632	3.894633
56	6	10.1526	-2.8799	-0.68704
57	6	11.87792	-3.1132	1.502228
58	6	11.51509	-2.89426	-0.87278
59	1	9.512313	-2.77715	-1.55223
60	6	12.39458	-3.03284	0.224905
61	1	12.5402	-3.21083	2.359719
62	1	11.92163	-2.79747	-1.87717
63	1	13.46899	-3.06892	0.0603
64	6	-1.69203	3.453075	0.00407
65	6	-2.84296	3.469606	-0.78828
66	6	-1.52447	2.413872	0.924822
67	6	-3.77258	2.447532	-0.69755
68	1	-3.01058	4.293859	-1.47526

69	6	-2.48919	1.436889	1.063123
70	1	-0.64359	2.372283	1.557254
71	6	-3.61801	1.412873	0.237702
72	1	-4.63626	2.465538	-1.356
73	1	-2.3508	0.676065	1.826024
74	6	-4.63457	0.35145	0.362021
75	6	-5.46965	0.020873	-0.70673
76	6	-4.80378	-0.35366	1.562303
77	6	-6.4776	-0.91922	-0.57051
78	1	-5.33391	0.491223	-1.67644
79	6	-5.82673	-1.27136	1.711732
80	1	-4.13989	-0.17681	2.404802
81	6	-6.70228	-1.55023	0.653376
82	1	-7.08297	-1.16715	-1.43708
83	1	-5.95277	-1.77032	2.667055
84	7	-7.82443	-2.45989	0.928031
85	6	-7.32289	-3.72438	1.462243
86	6	-6.14458	-4.35295	1.03784
87	6	-8.01753	-4.26729	2.551283
88	6	-5.54484	-5.32306	1.839865
89	1	-5.69513	-4.08143	0.086485
90	6	-7.41402	-5.23399	3.356318
91	1	-9.02435	-3.91844	2.766659
92	6	-6.13663	-5.70742	3.043959
93	1	-4.60984	-5.77926	1.521907
94	1	-7.93865	-5.60916	4.231991
95	1	-5.60399	-6.35661	3.735419
96	6	-9.38629	-1.067	-0.24331
97	6	-10.6089	-0.77816	-0.88422
98	6	-8.91628	-2.37071	-0.05725
99	6	-11.3639	-1.79786	-1.4166
100	1	-10.9461	0.255932	-0.93481
101	6	-9.63314	-3.45498	-0.71406
102	6	-10.8836	-3.13354	-1.36585
103	1	-12.3296	-1.59831	-1.87475
104	6	-9.20897	-4.81696	-0.81035
105	6	-11.6474	-4.16411	-1.98433

106	6	-9.95322	-5.77917	-1.45167
107	1	-8.26946	-5.12023	-0.38299
108	6	-11.1953	-5.46379	-2.03688
109	1	-12.6042	-3.89801	-2.42518
110	1	-9.57402	-6.79697	-1.51229
111	1	-11.7809	-6.23619	-2.52968
112	1	8.210334	-2.97524	4.305269
113	1	6.649405	-2.93053	2.373397
114	1	-8.82169	-0.23433	0.161061

Table S7. Coordinates of the optimized **(βND)$_2$-QCN** structure.

Center number	Atomic number	Coordinates X	Y	Z
1	6	-1.41867	-3.00788	-0.95836
2	6	-2.80937	-2.86964	-1.09037
3	6	-3.61663	-2.71774	0.06118
4	6	-3.02338	-2.70191	1.337757
5	6	-1.63271	-2.84003	1.46924
6	6	-0.83419	-2.99436	0.321065
7	1	-0.79937	-3.07395	-1.82701
8	1	-3.25314	-2.8253	-2.06123
9	1	-3.64019	-2.63333	2.206186
10	1	-1.18637	-2.88221	2.439835
11	6	-5.15536	-2.56239	-0.09409
12	6	-5.702	-1.27002	-0.13598
13	6	-7.3132	-3.49963	-0.28916
14	6	-7.86717	-2.19767	-0.34632
15	6	-8.17874	-4.63729	-0.31577
16	6	-9.28204	-2.03892	-0.48402
17	6	-9.5791	-4.46393	-0.44552
18	1	-7.78724	-5.63146	-0.24711
19	6	-10.1259	-3.17581	-0.5315
20	1	-9.72488	-1.0663	-0.55243
21	7	-5.97176	-3.6432	-0.22363
22	7	-7.04791	-1.12338	-0.27605
23	6	-10.5186	-5.68632	-0.50045

24	6	-11.6535	-3.01715	-0.67814
25	7	-11.2163	-6.59427	-0.54125
26	7	-12.7875	-2.89356	-0.78715
27	6	0.68324	-3.14654	0.467815
28	6	1.495728	-2.00011	0.542243
29	6	1.252852	-4.43181	0.521075
30	6	2.886867	-2.1379	0.654782
31	1	1.057316	-1.02931	0.474152
32	6	2.640084	-4.56909	0.676825
33	1	0.62671	-5.29631	0.488358
34	6	3.455896	-3.41764	0.721523
35	1	3.514364	-1.2761	0.672581
36	1	3.077247	-5.54151	0.759233
37	7	4.904408	-3.57268	0.861134
38	6	5.34975	-2.91365	2.093541
39	6	5.83602	-1.58789	2.0339
40	6	5.293647	-3.58987	3.323847
41	6	6.261595	-0.93923	3.208483
42	1	5.876917	-1.0735	1.095244
43	6	5.7169	-2.9408	4.49974
44	1	4.923013	-4.58596	3.362646
45	6	6.203906	-1.61765	4.442335
46	1	6.629825	0.060549	3.164561
47	1	5.671042	-3.4522	5.433006
48	1	6.525491	-1.12977	5.33427
49	6	5.777766	-4.27941	-0.08686
50	6	5.798206	-3.86581	-1.44098
51	6	6.563179	-5.32558	0.331139
52	6	6.603188	-4.50593	-2.35028
53	1	5.159903	-3.02536	-1.75116
54	6	7.406391	-6.00624	-0.58917
55	1	6.554441	-5.65434	1.381041
56	6	7.427269	-5.59204	-1.94608
57	1	6.625639	-4.19145	-3.40447
58	6	8.230733	-7.09256	-0.18582
59	6	8.270799	-6.27289	-2.86645
60	6	9.035976	-7.73258	-1.09505

61	1	8.208525	-7.40735	0.868311
62	6	9.056476	-7.31866	-2.44928
63	1	8.279507	-5.9442	-3.91648
64	1	9.674442	-8.57284	-0.7848
65	1	9.710067	-7.84749	-3.15854
66	6	-4.76678	-0.04741	-0.08892
67	6	-4.4516	0.542979	1.135243
68	6	-4.23473	0.469646	-1.27007
69	6	-3.60509	1.650592	1.178086
70	1	-4.87184	0.135573	2.066192
71	6	-3.38716	1.576987	-1.2273
72	1	-4.4829	0.004338	-2.23497
73	6	-3.07239	2.167581	-0.00351
74	1	-3.35712	2.116384	2.142888
75	1	-2.96748	1.984196	-2.15871
76	6	-2.13766	3.390534	0.044153
77	6	-0.77025	3.21539	0.258574
78	6	-2.65804	4.673273	-0.12714
79	6	0.076424	4.322841	0.302347
80	1	-0.36042	2.204031	0.394351
81	6	-1.8111	5.781094	-0.08437
82	1	-3.73572	4.811482	-0.29633
83	6	-0.44407	5.606103	0.130471
84	1	1.154153	4.184915	0.471977
85	1	-2.22161	6.792327	-0.21987
86	7	0.448583	6.773128	0.176582
87	6	-0.28759	7.93274	0.700272
88	6	-0.95752	8.787284	-0.17575
89	6	-0.31647	8.178699	2.072941
90	6	-1.65559	9.887895	0.32081
91	1	-0.93391	8.593536	-1.25795
92	6	-1.01553	9.279044	2.569899
93	1	0.211334	7.505186	2.763542
94	6	-1.68493	10.13369	1.694104
95	1	-2.18314	10.56186	-0.36967
96	1	-1.03847	9.472489	3.65227
97	1	-2.23545	11.00152	2.085398

98	6	1.779855	6.391531	-0.31637
99	6	2.443056	5.291205	0.279099
100	6	2.374375	7.089653	-1.33874
101	6	3.687101	4.910522	-0.1591
102	1	1.946042	4.748207	1.096485
103	6	3.662064	6.717073	-1.81237
104	1	1.867239	7.945882	-1.80793
105	6	4.326881	5.614515	-1.21607
106	1	4.209958	4.056817	0.297563
107	6	4.302633	7.42062	-2.86926
108	6	5.614804	5.241907	-1.68999
109	6	5.546617	7.039803	-3.3077
110	1	3.780089	8.274415	-3.32615
111	6	6.209689	5.939162	-2.7122
112	1	6.122079	4.385673	-1.22072
113	1	6.043486	7.582642	-4.12523
114	1	7.205793	5.653652	-3.08117

Table S8. HOMO, LUMO, S_1 and T_1 energy levels.

Compounds	HOMO (eV)	LUMO (eV)	E_g (eV)	S_1 (eV)	T_1 (eV)	ΔE_{ST} (eV)
αND-QCN	-5.26	-2.92	2.34	2.07	1.89	0.18
βND-QCN	-5.20	-2.95	2.25	2.00	1.84	0.16
$(\alpha ND)_2$-QCN	-5.15	-2.76	2.39	2.12	1. 98	0.14
$(\beta ND)_2$-QCN	-5.10	-2.78	2.32	2.05	1.94	0.11

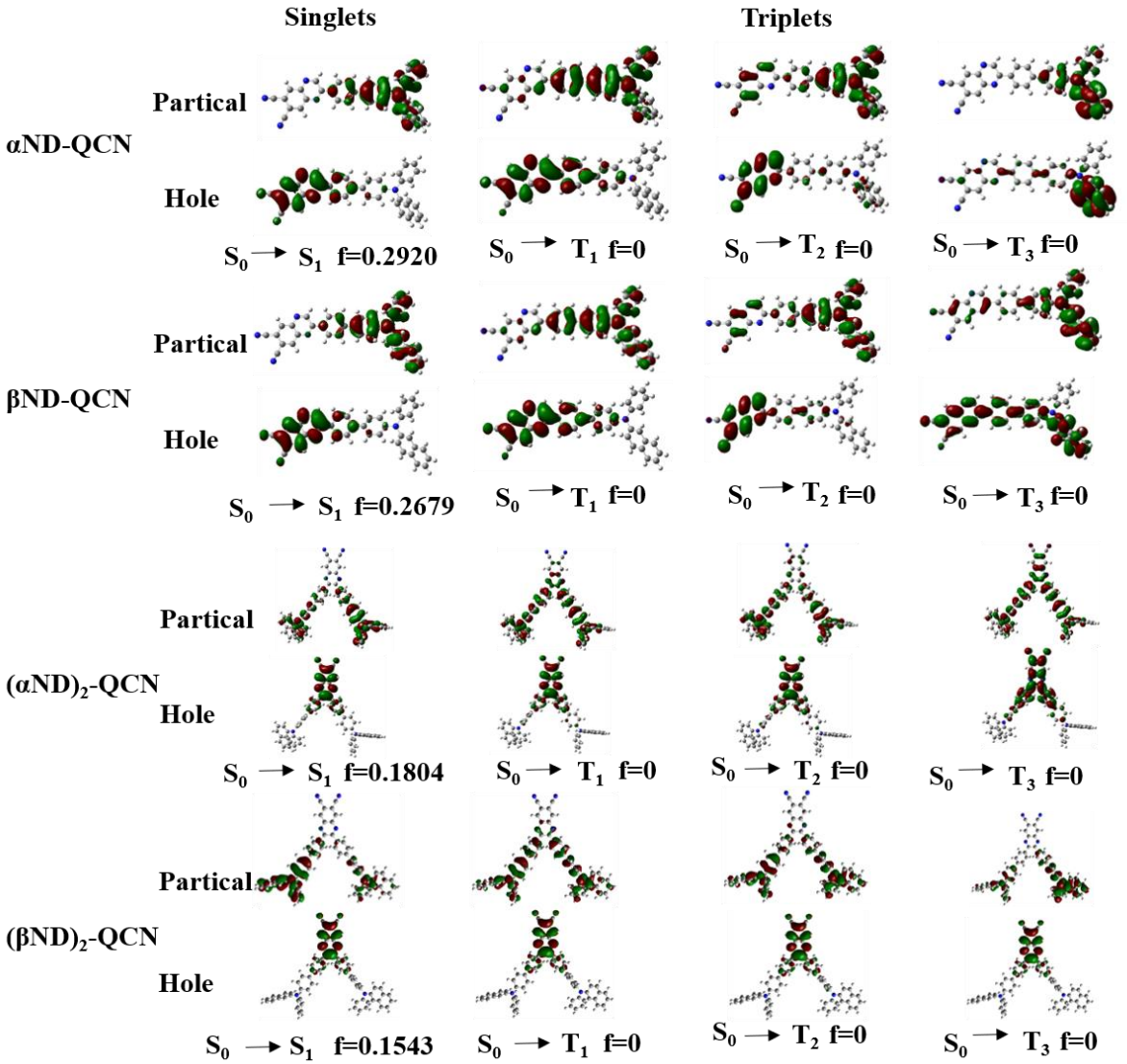

Figure S27. Natural transition orbitals for the $S_0 \rightarrow S_1$, $S_0 \rightarrow T_1$, $S_0 \rightarrow T_2$ and $S_0 \rightarrow T_3$ excitations in **αND-QCN**, **βND-QCN**, **$(\alpha ND)_2$-QCN** and **$(\beta ND)_2$-QCN**.

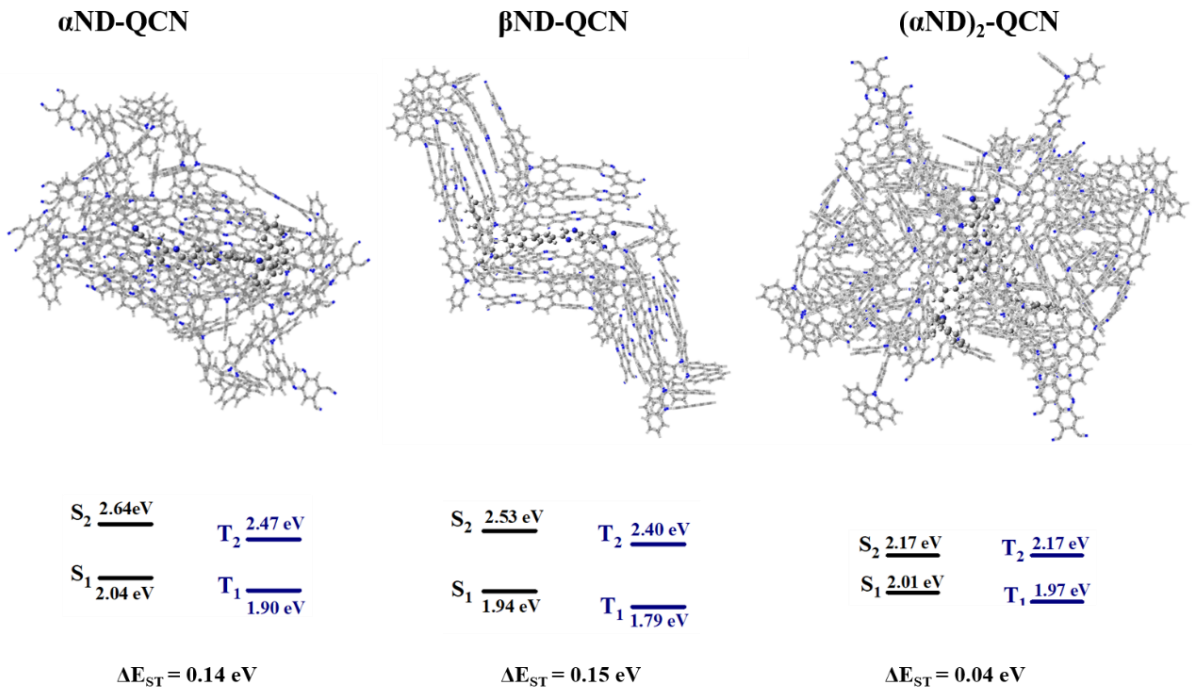

Figure S28. Gaussian ONIOM calculations of **αND-QCN**, **βND-QCN**, **(αND)$_2$-QCN** optimized geometries in the bulk matrix and the corresponding excited state energy levels.

7. Cyclic Voltammetry

Electrochemical measurements (cyclic voltammograms) were performed with a BAS 100W Bioanalytical electrochemical workstation, using glassy carbon electrode as working electrode, platinum wire as auxiliary electrode, and a porous glass wick Ag/Ag^+ as pseudo-reference electrode with standardized against ferrocene/ferrocenium. The oxidation and reduction potentials were measured in CH_2Cl_2 (DCM) solution containing 0.1 M of n-Bu_4NPF_6 in DMF as a supporting electrolyte at a scan rate of 100 mV s^{-1}.

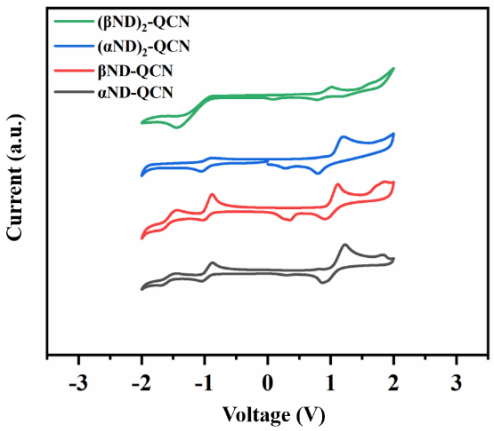

Figure S29. Cyclic voltammograms of **αND-QCN**, **βND-QCN**, **(αND)$_2$-QCN** and **(βND)$_2$-QCN**. The oxidation and reduction potentials were measured in DCM.

8. Device Fabrication and Performance

OLEDs were fabricated on the ITO-coated glass substrates with multiple organic layers sandwiched between the transparent bottom indium-tin-oxide (ITO) anode and the top metal cathode. Before device fabrication, the ITO glass substrates were pre-cleaned carefully. All material layers were deposited by vacuum evaporation in a vacuum chamber with a base pressure of 10^{-6} torr. The deposition system permits the fabrication of the complete device structure in a single vacuum pump-down without breaking the vacuum. The deposition rate of organic layers was kept at 0.1~0.2 nm s^{-1}. The doping was conducted by co-evaporation from separate evaporation sources with different evaporation rates. The current density, voltage, luminance, external quantum efficiency, electroluminescent spectra and other characteristics were measured with a Keithley 2400 source meter and an absolute EQE measurement system in an integrating sphere at the same time. The Hamamatsu C9920-12 system used for the EQE measurements was equipped with Hamamatsu PMA-12 Photonic multichannel analyzer C10027-02 whose longest detection wavelength is 1100 nm.

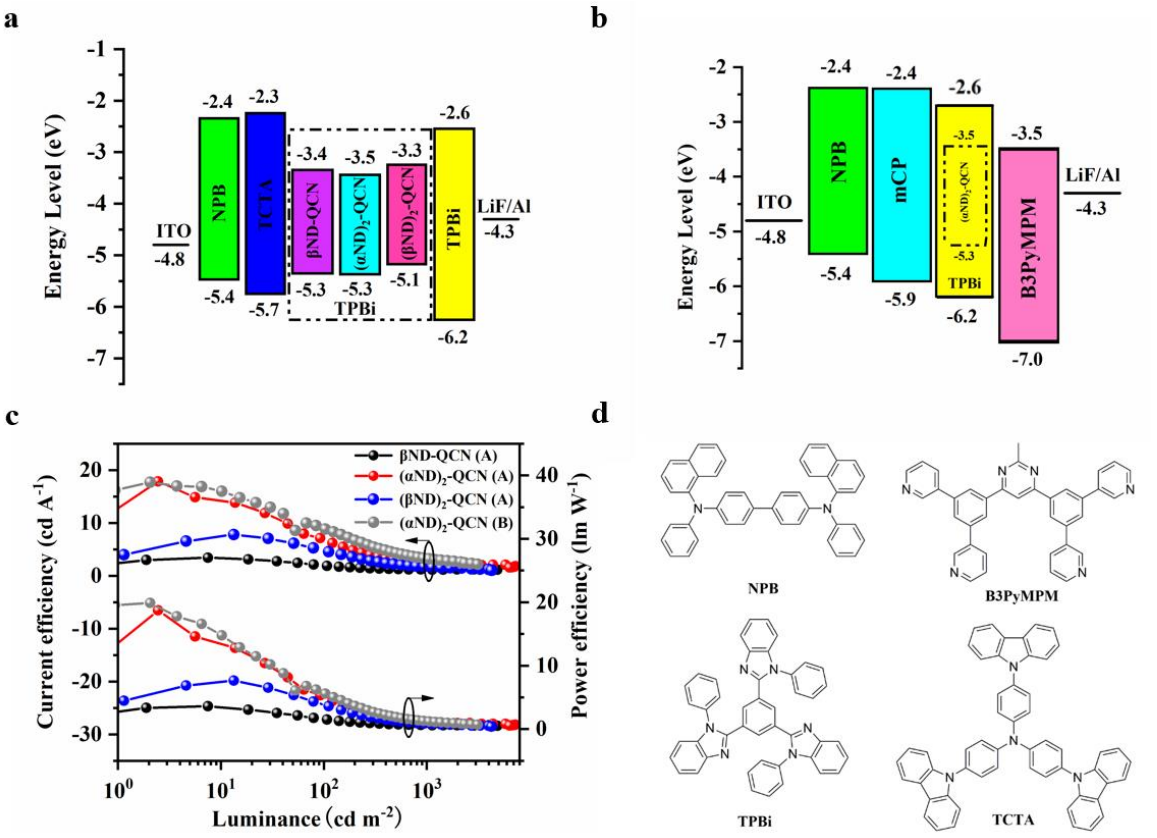

Figure S30. OLEDs based on QCN derivatives: (a) structure of device A; (b) structure of device B; (c) Current Efficiency-Luminance-Power efficiency plots of devices A and B; (d) molecular structures of the materials used in these devices.

Table S9. Summary of device performances of OLEDs based on **QCN**-derivatives

Emitters (device structure)	Doping concentration [wt.%]	λ_{ELmax} [nm]	L_{max} [cd m^{-2}]	CE [cd A^{-1}]	PE [lm W^{-1}]	EQE_{max} [%]	*CIE* (x, y)
βND-QCN (A)	10	617	4655	4.8	4.4	4.4	(0.58, 0.41)
	20	639	5579	4.1	4.1	5.8	(0.62,0.37)
(αND)$_2$-QCN (A)	10	594	5153	11.3	9.4	6.2	(0.51, 0.46)
	20	598	6247	12.0	11.1	7.6	(0.54, 0.45)
(βND)$_2$-QCN (A)	10	606	4357	6.9	5.6	4.6	(0.53, 0.45)
	20	623	4749	5.5	5.1	4.8	(0.58, 0.42)
(αND)$_2$-QCN (B)	15	630	4329	12.2	13.7	11.8	(0.60, 0.40)
	30	610	3130	17.7	19.9	14.3	(0.56, 0.44)

9. References

[1] C. Li, R. Duan, B. Liang, G. Han, S. Wang, K. Ye, Y. Liu, Y. Yi, Y. Wang, *Angew. Chem. Int. Ed.* **2017**, *56*, 11525.

[2] Y. Kanazawa, T. Yokota, H. Ogasa, H. Watanabe, T. Hanakawa, S. Soga, M. Kawatsura, *Tetrahedron* **2015**, *71*, 1395.

[3] A. Labrunie, J. Gorenflot, M. Babics, O. Alévêque, S. Dabos-Seignon, A. H. Balawi, Z. Kan, M. Wohlfahrt, E. Levillain, P. Hudhomme, P M. Beaujuge, F. Laquai, C. Cabanetos, P. Blanchard, *Chem. Mater.* **2018**, *30*, 3474.

[4] SADABS, Version 2012/1; Bruker, Bruker AXS Inc.: Madison, Wisconsin, USA **2012**

[5] G. M. Sheldrick, G. M. Found. Crystallogr., *Acta Crystallogr. Sect. A:* **2008**, A64, 112-122.

[6] Y. Chen, D. Zhang, Y. Zhang, X. Zeng, T. Huang, Z. Liu, G. Li, L. Duan, *Adv. Mater.* **2021**, 33, DOI: 10.1002/adma.202103293.

[7] Z. Yang, Z. Mao, Z. Xie, Y. Zhang, S. Liu, J. Zhao, J. Xu, Z. Chi, M. P. Aldred, *Chem. Soc. Rev.* **2017**, 46, 915.

[8] H. Uoyama, K. Goushi, K. Shizu, H. Nomura, C. Adachi, *Nature* **2012**, 492, 234.

[9] T. Vreven, K. S.Byun, I. Komáromi, S. Dapprich, K. Morokuma, M. J. Frisch *J. Chem. Theory Comput.* **2006**, *2* (3), 815–826.

[10] R. L. Martin, *The Journal of Chemical Physics*, ***2003***, *118(*11*), 4775–4777.*

[11] R. G. Parr, W. Yang, Density Functional Theory of Atoms and Molecules, Oxford University Press, Oxford, **1989**.

[12] R. Ditchfield, W. J. Hehre, and J. A. Pople *J. Chem. Phys.*, **1971**, *54*, 724.

[13] M. J. Frisch, G. W. Trucks, H. B. Schlegel, G. E. Scuseria, M. A. Robb, J. R. Cheeseman, G. Scalmani, V. Barone, B. Mennucci, G. A. Petersson, H. Nakatsuji, M. Caricato, X. Li, H. P. Hratchian, A. F. Izmaylov, J. Bloino, G. Zheng, J. L. Sonnenberg, M. Hada, M. Ehara, K. Toyota, R. Fukuda, J. Hasegawa, M. Ishida, T. Nakajima, Y. Honda, O. Kitao, H. Nakai, T. Vreven, J. A. Montgomery, Jr., J. E. Peralta, F. Ogliaro, M. Bearpark, J. J. Heyd, E. Brothers, K. N. Kudin, V. N. Staroverov, T. Keith, R. Kobayashi, J. Normand, K. Raghavachari, A. Rendell, J. C. Burant, S. S. Iyengar, J. Tomasi, M. Cossi, N. Rega, J. M. Millam, M. Klene, J. E. Knox, J. B. Cross, V. Bakken, C. Adamo, J. Jaramillo, R. Gomperts, R. E. Stratmann, O. Yazyev, A. J. Austin, R. Cammi, C. Pomelli, J. W. Ochterski, R. L. Martin, K. Morokuma, V. G. Zakrzewski, G. A. Voth, P. Salvador, J. J. Dannenberg, S. Dapprich, A. D. Daniels, O. Farkas, J. B. Foresman, J. V. Ortiz, J. Cioslowski, and D. J. Fox. EM64L-Gaussian 09, Revision D.01. Gaussian, Inc., Wallingford CT, **2013**.